The impact of induced airflow on the drying process of apples inside a solar drying chamber

A study on food preservation conducted in Nepal

Marion Karlsson Faudot

Master thesis in Energy and Building Design

Faculty of Engineering | Lund University

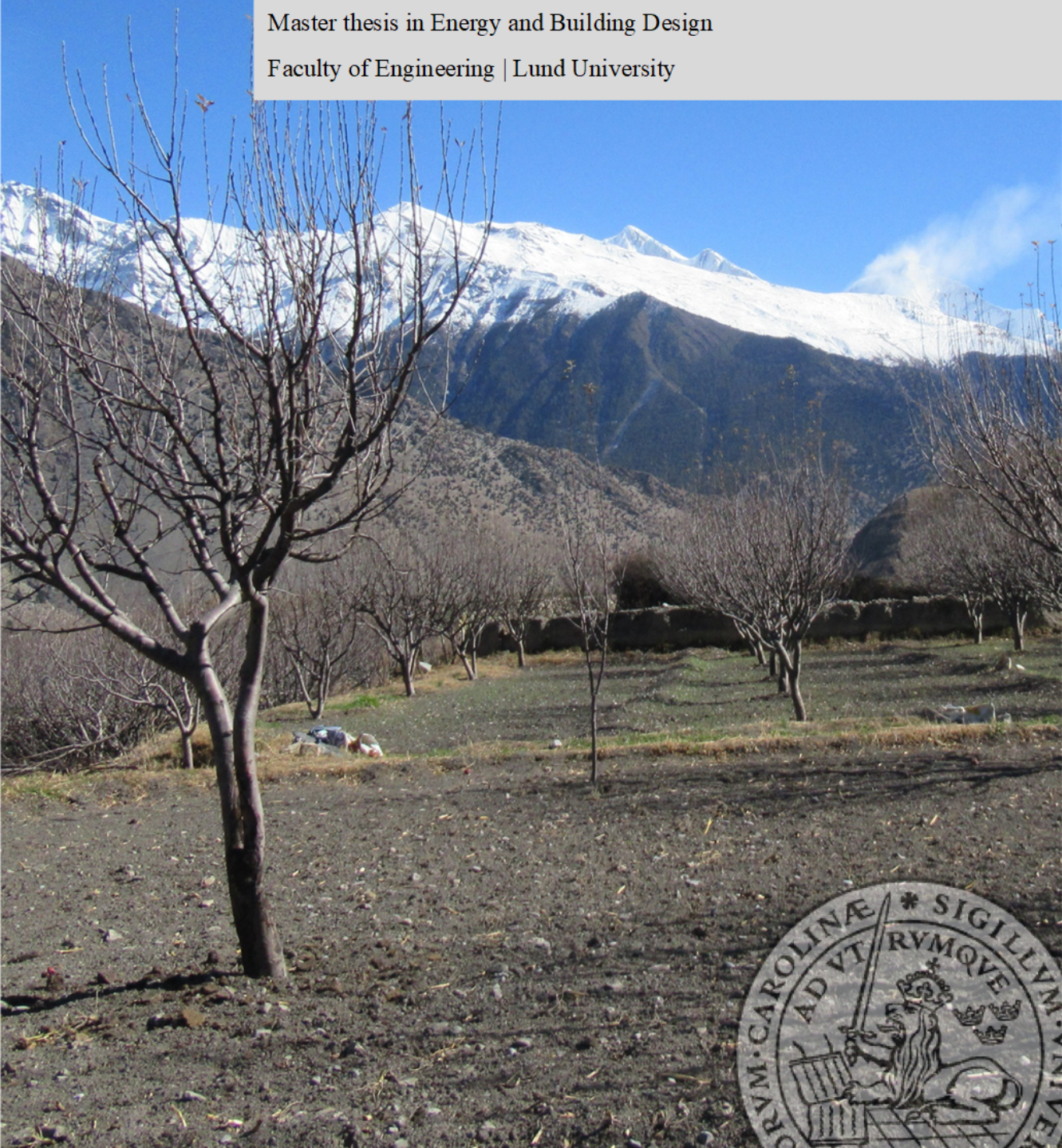

Lund University

Lund University, with eight faculties and a number of research centres and specialised institutes, is the largest establishment for research and higher education in Scandinavia. The main part of the University is situated in the small city of Lund which has about 112 000 inhabitants. A number of departments for research and education are, however, located in Malmö. Lund University was founded in 1666 and has today a total staff of 6 000 employees and 47 000 students attending 280 degree programmes and 2 300 subject courses offered by 63 departments.

Master Programme in Energy and Building Design

This international programme provides knowledge, skills and competencies within the area of energy-efficient and environmental building design in cold climates. The goal is to train highly skilled professionals, who will significantly contribute to and influence the design, building or renovation of energy-efficient buildings, taking into consideration the architecture and environment, the inhabitants' behaviour and needs, their health and comfort as well as the overall economy.

The degree project is the final part of the master programme leading to a Master of Science (120 credits) in Energy-efficient and Environmental Buildings.

Project

This master thesis is a part of the project 'SolarFood: Reducing post-harvest losses through improved solar drying' (VR-2020 -04071) funded by the Swedish Scientific Council in collaboration with the Swedish International Development Cooperation Agency. This project is being coordinated by Lund University (Dr. Martin Andersson and Dr. Henrik Davidsson).

Examiner: Ricardo Bernado, Ph. D (Energy and Building Design)

Supervisor: Dr. Henrik Davidsson (Energy and Building Design)

Co-Supervisors: Dr. Bivek Baral (Kathmandu University)
Dr. Martin Andersson (Division of Heat Transfer)
Paula Viola (Engineering and Nutrition)

Keywords: solar drying chamber, heat transfer, apples, fans, airflow, drying rate

Thesis: The impact of induced airflow on the drying process of apples inside a solar drying chamber - *A study on food preservation conducted in Nepal* (2022)

Abstract

To achieve food security around the globe, efficient food preservation techniques must be developed. This is especially true for Nepal, where low agricultural productivity due to poor technical knowledge, lack of irrigation and fertilisers as well as unstable weather patterns affect the welfare of the farming community.

This master thesis investigates how the internal air flow of a solar drying chamber can be manipulated to increase the heat transfer while maintaining an even drying process. Results show that placing an inlet on top of the drying chamber, combined with two internal fans gives the highest drying rate amongst performed experiments. If an even drying process is favoured, an inlet at the bottom of the chamber with one internal fan can be used. An increase in internal air flow ensures better heat transfer inside the drying chamber, reducing the drying time.

Future research should include possibilities of further improving the heat transfer and uniformity of the drying process by varying the net flow out of the drying chamber and by tuning the individual internal fans' air flow.

Acknowledgement

I would like to thank Dr. Bivek Baral and everyone in Nepal that I spent time with. You made me feel at home at Kathmandu University and gave me an incredible adventure to remember.

A special thanks to Dr. Henrik Davidsson, who did not only support me with the writing but also kept me motivated throughout these last months. Every time I felt that this thesis was not going anywhere you gave me the energy I needed to continue. I could not have wished for a better supervisor, so thank you from the bottom of my heart for giving me this opportunity and making my last course memorable.

Thank you mum, dad and Elise, for whom without I would not have made it to where I am today. I am also grateful to my friends for all the support they showed me, it was truly appreciated.

Table of content

1 Introduction **6**
- 1.1 Aim . . . 7
- 1.2 Research questions . . . 7

2 Background **8**
- 2.1 Previous experiments . . . 8
- 2.2 Drying rate . . . 9
- 2.3 Water activity . . . 10

3 Method **10**
- 3.1 Delimitations . . . 11
- 3.2 Design choice . . . 12
- 3.3 Setups . . . 14
- 3.4 Measurements . . . 15
- 3.5 Method optimisation . . . 18

4 Result **20**
- 4.1 Setup using inlet A: scenarios using the bottom inlet . . . 20
- 4.2 Setup using inlet B: scenarios using the top inlet . . . 26
- 4.3 Comparison between setup using inlet A and setup using inlet B . . . 33
  - 4.3.1 Temperature . . . 34

5 Discussion **37**
- 5.1 Optimal scenario making use of inlet A . . . 37
- 5.2 Optimal scenario making use of inlet B . . . 39
- 5.3 Optimal design . . . 39
- 5.4 Fan placement . . . 41
- 5.5 Potential method improvement . . . 42

6 Conclusion **43**
- 6.1 Future research . . . 43

References **44**

7 Appendix **46**
- 7.1 Calculation of the outlet's covered area for setup using inlet B . . . 46
- 7.2 Possible measurement error for airflow calculations . . . 46
- 7.3 Detailed lab instructions . . . 47
  - 7.3.1 Open experiment . . . 47

1 Introduction

The absence of efficient preservation techniques and storage facilities are an impediment for achieving food security around the globe. Solar dryers offer an environmentally friendly and cost effective way of preserving food while conserving the indigenous tradition of open sun drying (Andersson et al., 2020).

According to Federation of Nepalese Chambers of Commerce and Industry (2013), Nepal has the opportunity for high land productivity but settlements in the mountainous region experience food deficiency between four to nine months a year. Some of the reasons for the country's lack of agricultural productivity arise on account of poor technical knowledge, lack of irrigation and fertilisers as well as unstable weather patterns (Federation of Nepalese Chambers of Commerce and Industry, 2013). Moreover, Rose et al. (2021) mention that a lack of infrastructure makes transportation of goods to and from the mountainous regions difficult.

Nepal's Agricultural Research Council has worked on developing solar dryers to be used in remote and inaccessible areas of the country. A good preservation technique, such as drying, is of value for farmers that do not have the opportunity to sell fresh fruits and vegetables to the markets. Bhattarai (2018) mentions that selling dried food would facilitate transportation of the product and result in higher market prices. Higher market prices can be obtained for a product the later it is sold from its harvesting period, improving the economical welfare of the farmers. The ability for easy storage, through drying of nutriment, would also allow for a continuous supply of products in markets, even during the lean farming season (Bhattarai, 2018).

Implementing the use of solar dryers into Nepal's agriculture would help achieving the following United Nations Sustainable Development Goals (SDG):

- **No. 1: End poverty in all its form everywhere.** Increasing the quality of products through a more efficient drying technique results in increased product values. Dried crops have a longer shelf life than fresh crops which implies that the products can be sold off-season, further increasing their price (Andersson et al., 2020).
- **No. 2: End hunger, achieve food security and improved nutrition and promote sustainable agriculture.** The amount of waste that is spoiled due to the current inefficient drying technologies can be reduced. Having the possibility to conserve crops during an extended period makes the society less sensible to external factors that can otherwise result in a reduced harvesting period (Andersson et al., 2020).
- **No 3: Good health and well being.** Having an effective drying process ensures that nutritional values of dried crops are preserved (Andersson et al., 2020). Andersson et al. (2020) write that an effective drying process increase the availability of a wider range of products throughout the year.

- **No. 7: Ensure access to affordable, reliable, sustainable and modern energy for all.** Andersson et al. (2020) state that solar dryers use the sun as an energy source instead of biofuels or fossil fuels. By implementing solar dryers no additional source of energy is required for storage such as fridges or freezers, which helps keeping down costs of production and minimises the agricultural footprint on the environment (Andersson et al., 2020).

Previously, solar dryers have had a long drying time impacting food quality and taste (Andersson et al., 2020). A new innovative, socially integrated and efficient solar dryer that can be implemented at a large scale in Nepal is required to combat these issues.

1.1 Aim

The aim of this thesis is to enhance the heat transfer and create an even drying process inside the drying chamber of a solar dryer by focusing on its internal airflow. Having good heat transfer is of importance because it enables for the products to dry quicker, allowing for a high production rate. An even drying process is of equal importance to insure good product quality and results in less monitoring and work from the users' side. Not having to shift the drying trays around to make certain that all products are done drying simultaneously is time efficient. Additionally, an even drying process ensures that all nutrients are dried following guidelines inhibiting bacteria growth while retaining the products' nutritional values.

1.2 Research questions

To get an efficient design for a solar drying chamber multiple parameters are investigated. The first being the placement of the inlet, which supplies the drying chamber with heated air. The inlet and outlet tend to be placed at a distance from each other in order for the incoming air to pass through and disperse inside the drying chamber. If these two openings were to be next to each other the incoming air would not get a chance to spread throughout the chamber, resulting in short circuiting the airflow (figure 1.1a). When inducing airflow with the use of fans, it allows a certain degree of freedom regarding the placements of the inlet. In other words, the incoming air can be forced out of its natural trajectory towards the outlet (figure 1.1b). Being able to deviate the incoming air from its natural path by using fans results in an increased number of alternatives regarding the inlet placement, while mitigating the risk of short circuiting.

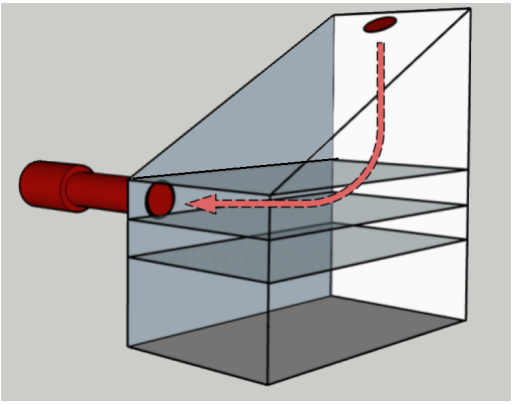

Figure 1.1a: Short circuiting of the airflow (red arrow) due to a badly placed inlet and outlet.

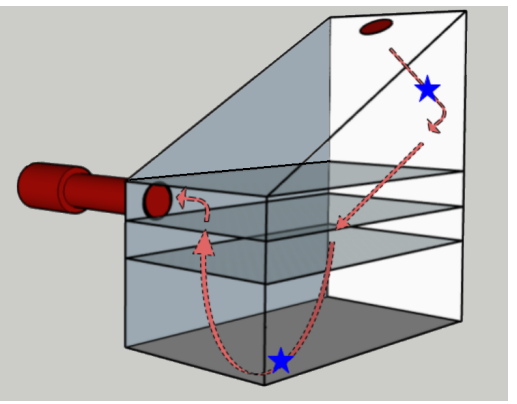

Figure 1.1b: Reducing the risk of short circuiting the airflow (red arrows) through the use of fans (blue stars).

Other parameters that are investigated to help design an efficient drying chamber are the optimal number, as well as the most favourable fan locations. Moreover, it is important to gain an understanding on how varying the airflow of the internal fans impacts the solar drying rate, as well as process. The parameters that are to be studied result in following research questions:

- Which inlet location result in a higher drying rate and even drying process?
- How many fans should be placed inside the drying chamber to increase the drying rate as well as get an even drying process?
- Where should the fans be placed in order to increase the drying rate and ensure an even drying process?
- How does different airflow of the fans placed inside the drying chamber impact the drying rate and drying process?

2 Background

2.1 Previous experiments

An experiment, which was conducted on an indirect flat plate solar collector using forced convection, shows that the drying time varies between the drying trays (Youcef-Ali et al., 2001). Furthermore, a study done by Nwakuba et al. (2016) reveals that the drying time decreases with the increase of air velocity. This study supports the findings of Castillo-Téllez et al. (2016), who deduces that drying chili at higher air velocity results in shorter drying time as well as lower final moisture content. An experiment conducted in 2007 by Fuller et al. (2007) on an indirect active solar dryer in the Humla Valley, Nepal concludes that, except for better hygiene and rain protection

there are no benefits in using solar dryers instead of traditional sun drying. For the sun dryers to match the traditional method, the drying trays have to be shifted every day to ensure that the air passes over or through them (Fuller et al., 2007). The calculated drying efficiency for the dryer in the experiment (13 %) is considered low for a forced convection dryer and this is attributed to the poorly distributed airflow through the collector and drying cabinet (Fuller et al., 2007). A recent experiment conducted in Bankariya, Nepal in 2020 on ginger shows that a mixed-mode dryer results in a shorter drying period (77.7 % time saved in comparison to manual drying) (Basnet et al., 2020). The study also concludes that using a fan to create forced convection could increase the drying rate even further (Basnet et al., 2020).

These experiments mention the potential that additional induced airflow can have on the drying rate. However, they do not investigate further how this can be optimised to increase solar dryers' efficiency. This thesis aims to explore the potential that induced airflow has on the drying process.

2.2 Drying rate

Drying curves show how the drying rate changes with time (figure 2.1).

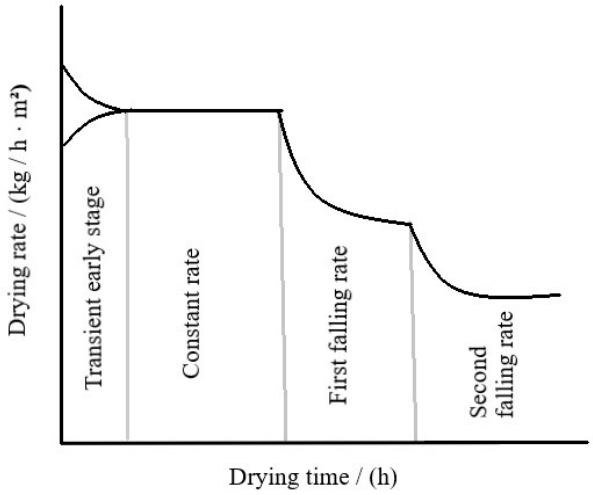

Figure 2.1: A typical drying rate curve showing the drying rate versus drying time. (Inspired by: Shafiur Rahman and Perera (2007))

Typical drying curves display the presence of three different phases during the drying of a product. In the transient early stage the product is heated up. The next stage is the constant rate period, where the moisture does not encounter internal or external mass transfer resistance and evaporates. In this stage the drying is controlled solely on external heat transfer. The third stage is the falling rate, which is characterised by a slowing down of the drying rate. This occurs due to the remaining water in the product being tightly bound. Two falling rates can sometimes be observed and it is hypothesised

that the first falling rate stage is controlled by internal and external mass transfer rates. It is hypothesised that the second falling rate is depended only on internal mass transfer resistance. Figure 2.1 shows a typical drying curve behaviour. It should be highlighted that drying behaviour of nutriments correlate with the product's porosity, homogeneity and tendency to absorb moisture from the surrounding air. (Shafiur Rahman and Perera, 2007)

2.3 Water activity

Water activity is used as an indicator for the availability of water that microorganism can use. Reducing this value helps diminish microbiological growth in products. (Swedish Food Agency, 2021) Water activity is measured on a range of 0 to 1, where 1 indicates that all water in the product is available to microorganisms. Bacteria require a higher water activity than yeasts and molds. While fresh fruits and vegetable have a water activity of around 0.95 to 0.99, dried nutriments range between 0.6 to 0.85. Figure 2.2 shows in what water activity range different types of microorganisms in food reproduces. (Rosengren, 2017) In the study conducted by Dong Chen and Patel (2008), the water activity is measured by estimating the relative humidity of air in equilibrium with a nutriment sample put in a sealed chamber. Dong Chen and Patel (2008) support Rosengren (2017) and both claim that no microbial growth is expected at water activity levels below 0.6. According to the institution of Food Technology at Lund University, the temperature range for drying food should be between 50 °C to 65 °C to inhibit microbial growth and minimise degradation of vitamin C. (Bengtsson and Döhlen, 2016) More specifically, Tiwari et al. (2016, chapter 12) state that the maximum allowable temperature for drying apple is 70 °C.

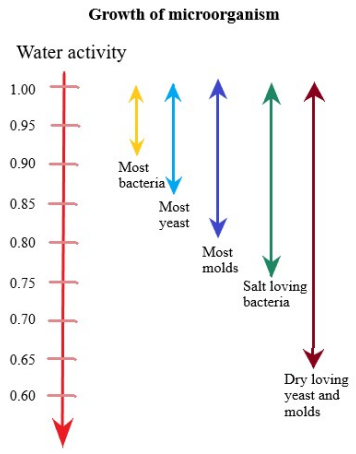

Figure 2.2: The range of water activity at which different types of microorganisms can reproduce. (Inspired by: Rosengren (2017))

3 Method

The empirical data had a qualitative approach and was used to compare the different scenarios presented in chapter 3.3. The research questions mentioned in chapter 1.1 were not answered individually since an efficient drying chamber design which simultaneously combines the following four parameters was to be found: (1) inlet location, (2) number and (3) placement of fans as well as (4) fans' airflow. To avoid testing all possible outcome and save time, as well as money, the number of experiments conducted was minimised. Through a good method optimisation a result could be found, without having to test all combination of parameters and every possible

placement of the fans. How the optimisation was conducted can be read in chapter 3.5. When following the method optimisation the risk of finding a local maximum instead of global maximum increases. It is therefore important to be transparent and clarify why certain experiments were deemed fit to dismiss.

3.1 Delimitations

Measurements were conducted on a setup that aimed to mimic the drying chamber of a solar dryer. By focusing solely on the drying chamber multiple uncertainties in the measurements were removed, e.g variability caused by the absorber. This also removed the requirement of measuring the ambient environmental parameters. Environmental parameters such as wind direction and solar irradiation became irrelevant since the input variables were regulated manually. Air leakages caused by slits in the construction were neglected since the prevailing leakages was considered small in relation to the exiting airflow. Even if results produced were not subject to natural conditions, they were deemed valid to use in a comparative manner to investigate different potential design for the drying chamber.

During the experiments it was not possible to weigh all the samples due to time constraints. To get an overview of how the drying process acted across the drying chamber each tray was divided into three sections. Five selected pieces per tray, with at least one located in each section, were chosen as observation samples to create drying rate curves. Sample selection depended on the inlet placement but remained the same indifferent to the number and placement of the internal fans. This enabled to see if improvements were reached at the various locations inside the drying chamber during different scenarios.

To display how the drying rate (equation 3.1) changed with time, the chamber had to be opened to conduct the required measurements. To avoid repeated decrease in temperature throughout the experiment it would have been preferable to track the samples' weight change inside the drying chamber without having to open it. In order to get readings of the drying rates and temperatures under undisturbed conditions some of the experiments were conducted through closed door.

It was speculated that the results would be affected by the amount of products in the drying chamber since sample pieces saturate and hinder the air. This was tested by conducting some experiments with 24 sample pieces per tray and some with 50 sample pieces per tray. The experiments containing 50 samples were invariably conducted behind closed doors to ensure pristine conditions inside the chamber. If during these experiments the chamber had been opened, the heavily saturated air would have been removed. Hence, the effect that a loaded chamber had on the drying conditions would not have been accurately described.

Lastly, investigating the health aspects of the dried samples laid outside of the scope of this thesis. In this case the health aspects referred to having hygienic drying conditions

that ensured the products retained their nutritional values and were safe to consume.

3.2 Design choice

The inside measurements of the drying chamber on which the experiments were conducted can be seen in figure 3.1. The chamber had a volume of approximately 0.29 m^3. The drying chamber was made from plywood as it was inexpensive and easy to acquire. In addition to the previously mentioned benefits, wood is a poor conductor of heat (Folaranmi, 2008). Using plywood therefore contributed to reducing the chamber's heat losses. Some of the disadvantages with using wood as a material was that it easily absorb water which makes it expand, certain fungi and insects digest it making it deteriorate and it is combustible (Team Engineering, 2019). To avoid the material from absorbing water and further reducing heat losses it is possible to line the inside of the drying chamber with aluminium foil, like what was done in the experiment preformed by Folaranmi (2008). However, due to the project's experiments being conducted within a small time frame, the deterioration state of the material was not an eminent concern. Therefore, the drying chamber was not lined with aluminium foil, even if it could have enabled further reduction of heat losses. To insure reduced heat losses and that a desirable drying temperature was reached, the outside of the drying chamber was fitted with polystyrene sheets with a thickness of 5 cm. Fastening the insulation with glue proved to be insufficient which resulted in the polystyrene sheets being taped together at the edges to minimise heat losses.

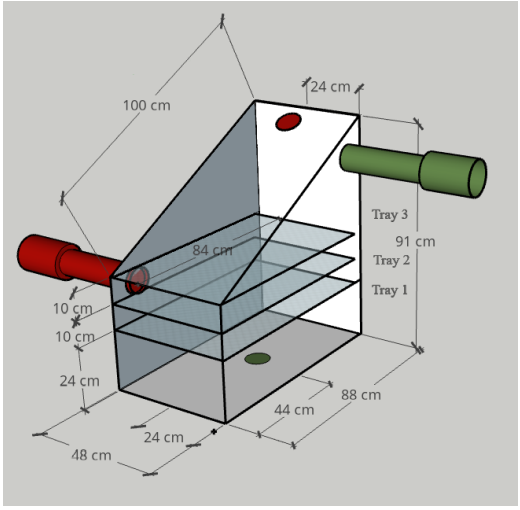

Figure 3.1: Diagram of the inside measurements and tray numbering of the drying chamber on which measurements were conducted.

The choice of the drying chamber's geometry originated from the design of a solar thermal dryer being tested in a parallel experiment (figure 3.2). By having replicated the shape that the drying chamber would have if implemented in the solar thermal dryer more relevant results were collected. The tilt angle of the chamber's lid was set to 28°. The reason for this value came from a study conducted by Shakya et al. (2019). The report concluded that

the optimal tilt angle for the month of October was 27°and for the month of November, as well as December, was 28°. Matching the tilt angle of the drying chamber's lid to that of the absorber on the solar thermal dryer made the experimental setup more authentic to real life.

The placement of the inlets that were tested were located at the centre of the bottom plate (green circle in figure 3.1) and at the top of the drying chamber (red circle in figure 3.1). The green inlet was chosen to be tested since common designs of indirect solar dryers, such as the ones used in the experiment conducted by Basnet et al. (2020) and Fuller et al. (2007), let the air enter from the bottom of the drying chamber to utilise natural convection. Placing the green outlet at a high point enabled the air to pass through the chamber with minimum assistance from fans. The location of the red outlet was selected to replicate the setup of the solar dryer being tested in a parallel experiment (figure 3.2). The reason for its corresponding inlet being centred and towards the highest situated edge of the lid was to allow for the absorber to heat up the air before letting it enter the drying chamber.

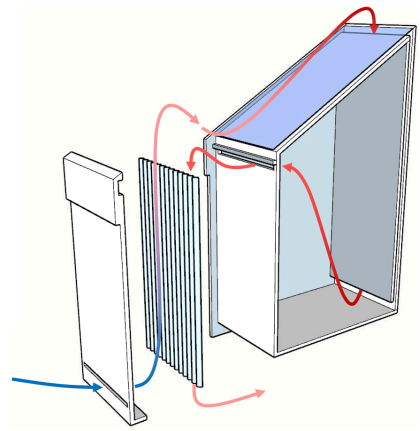

Figure 3.2: The design of the solar dryer on which the drying chamber's geometry is based on (Probert, 2021). The ribbed sheet is a heat exchanger and the arrows indicate the direction of the airflow. The blue and red colour scheme shows the gradual increase of the air's temperature.

The inlet tube was a galvanised and detachable iron pipe and the inlet holes were resealable. This enabled movement between the two test locations presented previously. The tube had heating lamps placed inside of it to allow control of the incoming air's temperature. To hold the heating lamps in place fine mesh wire was used. The inlet tube's length (52 cm + 12 cm) was kept short to reduce heat losses while still allowing enough space to accommodate the heat lamps. The galvanised metal outlet tube was suited with a fan, pulling air through the chamber (green and red tubes in figure 3.1). This external fan was set to a voltage between 2.1 V to 2.3 V. The outlet tube (105 cm + 17.5 cm) had a minimum unobstructed length of 70 cm to allow measurement of air velocity to be taken according to the standard written by Johansson and Svensson (1999). The inlet and outlet holes both had a diameter of 10 cm, implying an area of approximately 79 cm^2.

Figure 3.3a: A stand used to attach a fan when using the bottom inlet (green circle in figure 3.1). The space between the fan and the wall is of 5 cm to 5.5 cm.

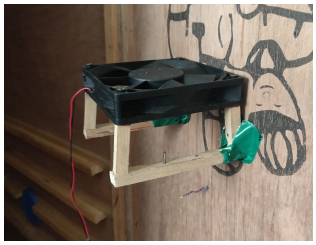

Figure 3.3b: A stand used to attach a fan when using the top inlet (red circle in figure 3.1).

The fans inside the drying chamber were attached on stands (figure 3.3a, 3.3b). If multiple fans were used they were connected in parallel to ensure that they had the same voltage across them. The trays in figure 3.1 were drying trays labelled from one to three. In two previously conducted studies by Islam et al. (2018) and Papade and Boda (2014) the choice of tray material ensured that air circulation inside the drying room could occur. To comply with this, the drying trays were made from a wooden frame and covered with fine mesh metallic net. Kendall et al. (2004) mentioned that it was not ideal to use metal trays since they can corrode or discolour the nutriment and recommend lining them with for instance cheesecloth. However, since the health aspect of the drying process was not in focus, a fine mesh metal net was used as tray material. To further facilitate air circulation Kendall et al. (2004) advised that the trays should be 4 cm smaller in both length and width than the drying room and 5 cm apart when stacked. To ease the tray mobility and taking measurements the trays were placed with 10 cm apart. To simplify the design only the length and not the width of the trays were 4 cm shorter than the drying room. Moreover, the outlet marked as a red pipe in figure 3.1 was located in between tray 2 and tray 3 to mitigate the impediment of the air exiting the drying chamber. It should be noted that the tray did obscure approximately 11 % of the air's entry point (appendix 7.1).

3.3 Setups

The scenarios tested during the different experimental runs were referred to with: α:β:γ. α being the position of the inlet (**A** or **B**), β being the number of fan (**0**, **1**, **2** or **3**) and γ being the voltage used by the fan(s) inside the drying chamber.

A : This setup used the bottom inlet (figure 3.4a).

B : This setup used the top inlet (figure 3.4b).

0 : The scenario in which no internal fans were added to the drying chamber. This scenario was only tested using the bottom inlet since it could be assumed that using the top inlet without any fans would result in short circuiting of the airflow (figure 1.1a).

1 : The scenario which made use of 1 fan inside the drying chamber.

2 : The scenario which made use of 2 fans inside the drying chamber. The location of the first fan was not moved.

3 : The scenario which made use of 3 fans inside the drying chamber. The locations of the two previous fans were not altered.

* 2.1 V
* 4.2 V
* 9 V
* 12 V

Figure 3.4a: Experimental setup which used inlet A (green arrow).

Figure 3.4b: Experimental setup which used inlet B (red arrow).

3.4 Measurements

The variables measured were the temperature at various locations, the outgoing air velocity and the relative humidity (RH) exiting the chamber (figure 3.5). Additionally, the water activity for the congregated samples for each individual tray was measured. The combined weight of the samples from each tray section (figure 3.7) was tabulated and their initial active surface area was recorded. These values were taken to enable calculation of the drying rate (equation 3.1). During the drying period of some experiments the chamber was opened and the weight of specific samples were noted (figure 3.7). Detailed instructions on how the experiments were conducted can be viewed in appendix 7.3.

The temperature inside the drying chamber was measured using type T thermocouples, set to measure from -270 °C to 180 °C*. The thermocouples were used together with a Campbell Scientific CR1000 data logger and AM16/32 multiplexer. The placement of the thermocouples are represented as crossed circles in figure 3.5. The thermocouples were

*For scenario **B:2:12**, conducted on 24 samples and on 50 samples, and scenario **B:2:9** the program was rewritten to give more accurate results. In these cases the thermocouple at the inlet was set to measure from -270°C to 180 °C while the remaining thermocouples were set to measure from -46 °C to 78 °C.

situated in the middle of each side and between the trays (i.e they were placed at 5 cm above each tray). The program written for the Campbell Scientific CR1000 data logger ensured that one measurement was taken every minute.

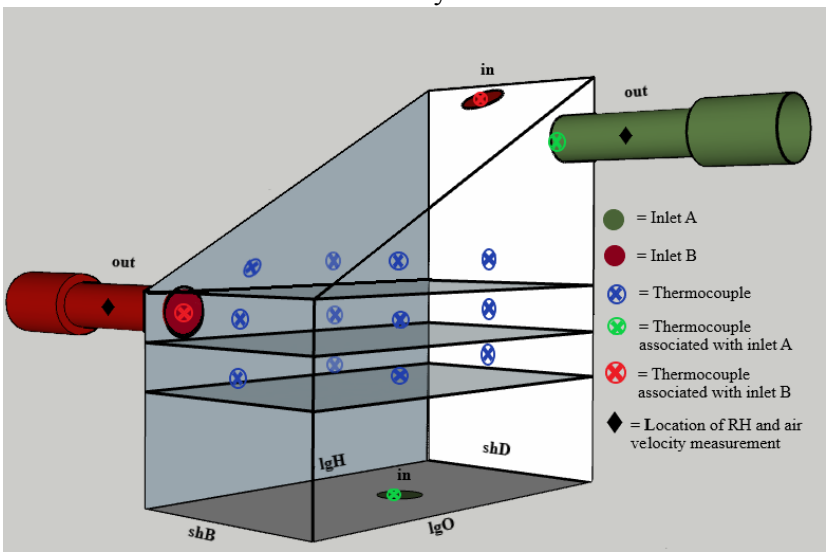

Figure 3.5: A diagram showing the placement of the thermocouples used to record the temperature, the measuring location of the air velocity and RH, as well as the naming of the dryer's side.

The air velocity measurements were conducted using a thermal anemometer and followed the measuring method described by Johansson and Svensson (1999). This standardised measuring method gave instructions on how to conduct proper velocity measurements, but also on how to validate the measurement plan. During the validation of the measurement plan the occurrence of regurgitation in the outlet pipe using a Prandtl tube was not tested. Having placed a fan in the outlet tube which purpose was to pull the air out of the drying chamber made the occurrence of regurgitation improbable, which rendered this test dispensable. Johansson and Svensson (1999) stated in their method description that a thermal anemometer should not be used for measurements below 0.5 m/s. This was disregarded as the instrument used (Testo velocity probe 0635 1535), which had an accuracy of $\pm$ 0.3 m/s + 4 % measured value, was solely utilised to approximate the dryer's environment. These measuring values were not used as a fundament for the conclusions, rendering the error margin arising from the accuracy of the instrument trivial.

The Testo velocity probe, originally calibrated for the reference temperature 1013 hPa, was compensated with a correction factor of 1.206. This being the median correction factor obtained from the instrument's manufacturer, which was representative for the air pressure in Dhulikhel, Nepal. Following the standard given by Johansson and Svensson (1999) the measured airflow was not only compensated for by the instrumental correction factor (1.206) but also with a correction factor of $k_1 = 0.96$. The correction factor k_1 was used to compensate for the shape of the canal on which the measurement were conducted.

The methodological error, which amongst other things can be attributed to the tilting of measuring equipment, was between 4 % and 6 %. A possible measuring error due to calibration mishaps judged minor and not considered in this thesis can be read about in Appendix 7.2. Furthermore, the standard set by Johansson and Svensson (1999) required that the length of undisturbed flow was of at least 50 cm prior to the measurement location and of minimum 20 cm post the measurement location. For these experiments, a distance of 55 cm prior and of 39 cm post the measurement location were used. Duct tape was used to reseal the opening after measurements.

The RH was measured using a Testo air velocity probe with an accuracy of $\pm$ 2 % for RH values between 2 % and 98 %. The RH measurement point was taken at the centre of the outlet's cross section and at the same location as the flow measurements. The water activity was measured before and after the experiments using the method described in chapter 2 by Dong Chen and Patel (2008). For this reason, a sealable container together with a temperature and moisture logger (TML) with USB was used. The TML had an accuracy of $\pm$ 3 % for RH readings around 50 % and was programmed to take 50 sample points at intervals of 10 seconds.

In this project the drying rate was defined as the amount of water evaporated per unit time and active surface area (equation 3.1). Red apples were chosen as test samples and when available the same brand of apples were bought. In case of product deficiency similar produce was selected. These were cut without removing the core, using a mandolin slicers set to a thickness of 0.3 cm (figure 3.6). When weighting the apples a Kern Analytical balance ABJ 220 - 4 NM with a reproducibility of 0.2 mg was used. The active surface area prior to drying was used to calculate the drying rate. To measure the samples' active surface area the slices were assumed to be circular and a tape measurement was used to evaluate their diameter. When the pieces were uneven the longest side was defined as the diameter. Selecting the longest side as the diameter ensured that the drying rate was underestimated rather than overestimated. The time period lapsed from when the samples were removed from the drying chamber was used to calculate the drying rate (equation 3.1). The weighting of samples took up to 15 minutes and it was presumed that the slices cooled rapidly. This led to an overestimation of the drying rate, albeit less exaggerated than if continuous drying throughout the weighting period was assumed.

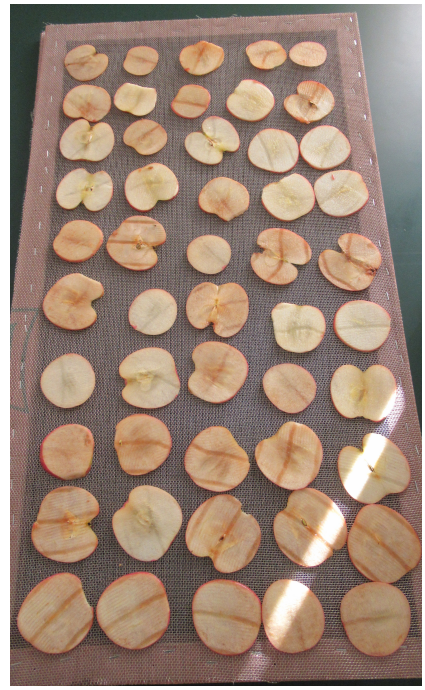

Figure 3.6: A tray filled with 50 slices of apples, each of a thickness of 0.3 cm.

$$\text{Drying rate} = \frac{\Delta\text{mass}}{\text{time} \cdot \text{initial active surface area}} \qquad [\text{g} / (\text{h} \cdot \text{m}^2)] \qquad (3.1)$$

The location of the selected samples weighted during experiments in which the drying chamber was opened varied depending on the inlet used and can be seen in figure 3.7.

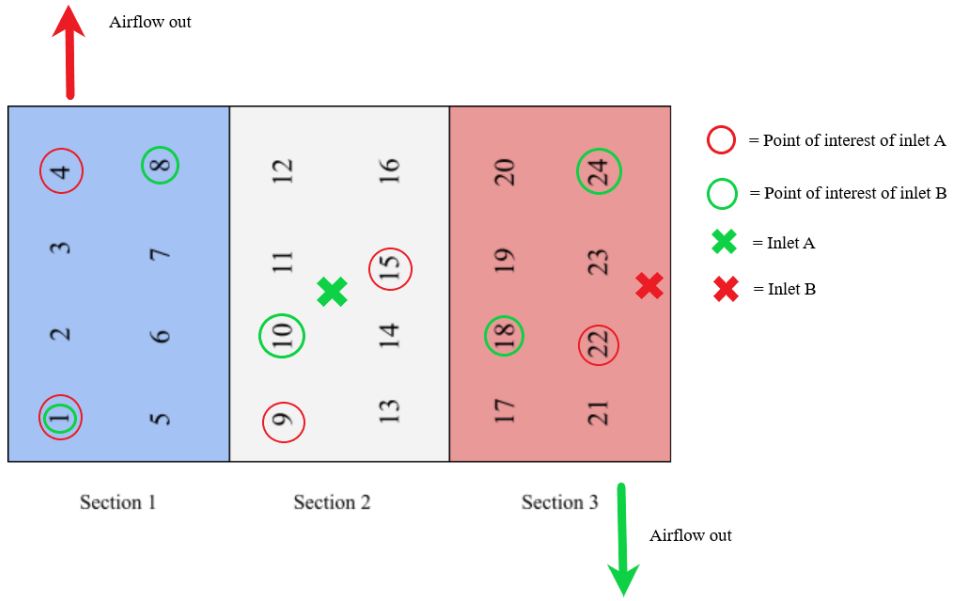

Figure 3.7: The points of interest looked at during experiments where the drying chamber was opened. The exact placement of the inlets can be seen in figure 3.1.

The first selected point of interest was at the centre of the drying chamber (sample 10 and 15). The second point was located near the outlet (samples 4 and 18) and the third laid near the inlet of respective setup (samples 10 and 22). The next observation site was selected with the characteristic of being as far away from the inlet as possible (samples 1 and 24). The final location to monitor was chosen from an area not previously covered by any of the other points of interest (sample 8 and 9). Spreading out the samples to survey allowed to get an overview of the trays' drying rate. It was presumed that sample pieces located beside each other did not differentiate in a significant way and were therefore not selected as point of interest.

3.5 Method optimisation

To find the number of fans, their respective placement and airflow which resulted in the highest drying rate and most even drying process without testing all possible outcome, the optimisation flowchart below was used (figure 3.8).

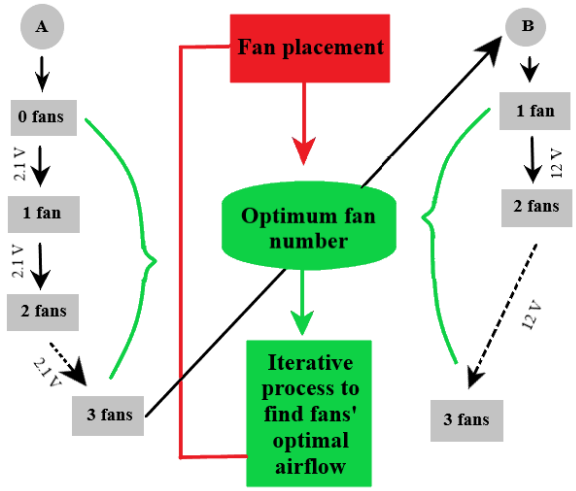

Figure 3.8: Flowchart showing the order to conduct the experiments to be time efficient.

The first scenario tested was **A:0** so that all other results could be compared to a inexpensive, simple and traditional design. Scenario **A:1:2.1** and **A:2:2.1** were investigated to see if a noticeable increase in drying rate could be observed. If the experiments showed similar results then **A:3:2.1** was not tested. On the other hand, if a significant difference in result occurred, **A:3:2.1** was investigated. Same process was conducted for scenario **B:1:2.1** and **B:2:2.1**.

Once the number of fans for both inlets which corresponded to the most efficient drying process was labelled ($\beta_{\mathbf{optimal}}$), the experiments were repeated but for different γ values. This to give an indication on the impact that the airflow of internal fans had on the drying rate. The intention was to find the lowest flow which resulted in a high drying rate while encouraging an inexpensive solar dryer design. Through an iterative process an approximation of the optimal flow ($\gamma_{\mathbf{optimal}}$) for the scenario α:$\beta_{\mathbf{optimal}}$: was found.

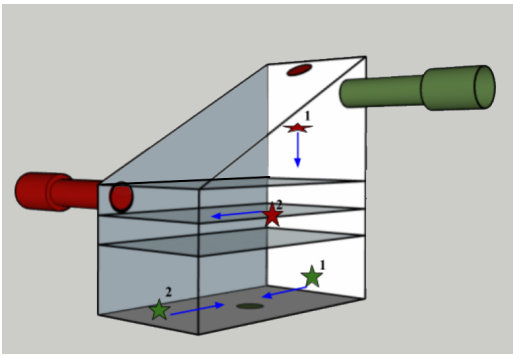

Figure 3.9: A diagram of the initial placement of the fans for the setup using inlet A (green stars) and the setup using inlet B (red stars). The numbering corresponds to the order of the fans placement. The blue arrows indicate the direction at which the fans blow.

Lastly, the placement of the internal fans were optimised. The fans' initial positions can be seen in figure 3.9. Using each of the inlets' optimal number of fans and airflow setting (α:$\beta_{\mathbf{optimal}}$:$\gamma_{\mathbf{optimal}}$) the fans were moved around. If a significant improvement in the drying rate and drying

process was attributed to the placement of the fans, they were moved around until the optimal placement for respective inlet was found. If one of these newly found position yielded a major advantage then that setup was tested again with an inferior number of fans. If a similar or improved drying process was observed with the new placement and with an inferior number of fans, the iterative process to find the fans' optimal airflow was conducted again. The reason for this was because an affordable and simple design was favoured.

4 Result

In this chapter the RH and outgoing airflow for multiple experiments is presented and the drying rate of the trays' sections for different scenarios post drying is shown. In order to discuss the evenness of the drying process, the integrated drying curves for the divergent points of interest after four hours of drying are displayed. The water activity levels for different experiments, prior to and post drying, are shown. Lastly, temperature graphs are presented to help support the discussion conducted in chapter 5.

Before presenting the result it is important to highlight a couple of things. Firstly, the starting value of RH and airflow for scenario **A:0_24.samples**, **A:2:2.1_50.samples**, **A:2:4.2_50.samples** and **B:2:12_24.samples** are taken prior to the trays being placed inside the drying chamber and are considered outliers. When analysing the data these values are disregarded (dashed lines in figure 4.1a, figure 4.1b, figure 4.5a and figure 4.5b). Secondly, it is of importance to note that the measurements are taken during different surrounding conditions. This implies that the RH values should be seen as relative to one another. Furthermore, even if the room temperature at the start of each experiment is invariably between 14 °C and 16 °C, the ambient temperature undoubtedly varied throughout the day. However, the experimental setup being located inside a room, away from direct sunlight, makes the variation small enough to assume insignificant. Lastly, the external fan's voltage is increased from 2.1 V to 2.2 V for scenario **A:2:2.1_50.samples** and to 2.3 V for scenario **A:2:4.2_50.samples**. The latter setting is kept throughout the experiments conducted on inlet B. The reason being that during power shortages the external fan would stop and not automatically restart and so the voltage had to be increased to resolve this issue. The external fan's voltage is changed by a maximum of 0.2 V, which is deemed small enough to not have a significant effect on the net flow out of the chamber nor majorly affect the result.

4.1 Setup using inlet A: scenarios using the bottom inlet

The prevailing conditions of the drying chamber for different experiments and throughout eight hours of drying is seen in figure 4.1.

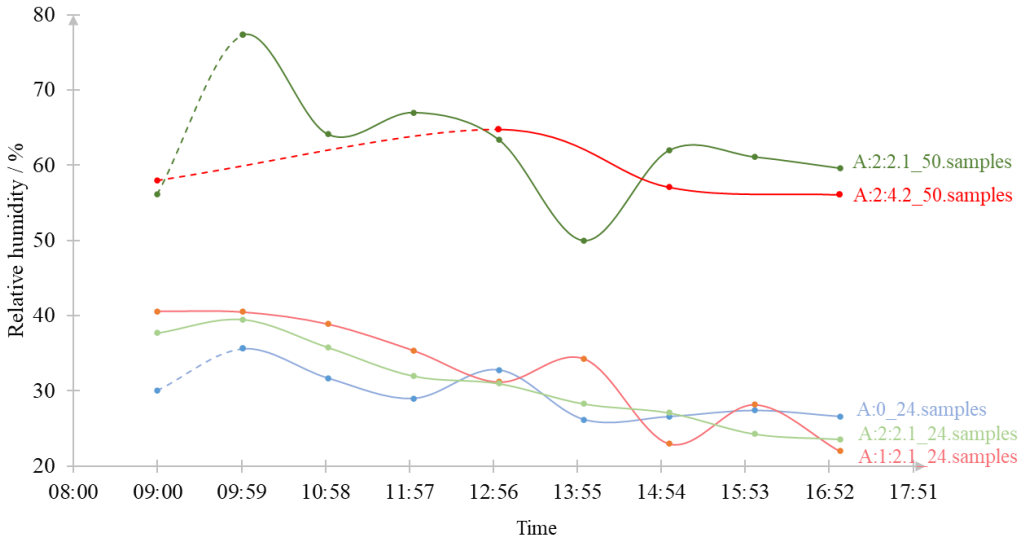

Figure 4.1a: The change of RH humidity in the outgoing air with respect to time for different scenarios making use of inlet A. The dashed lines represent outlier data.

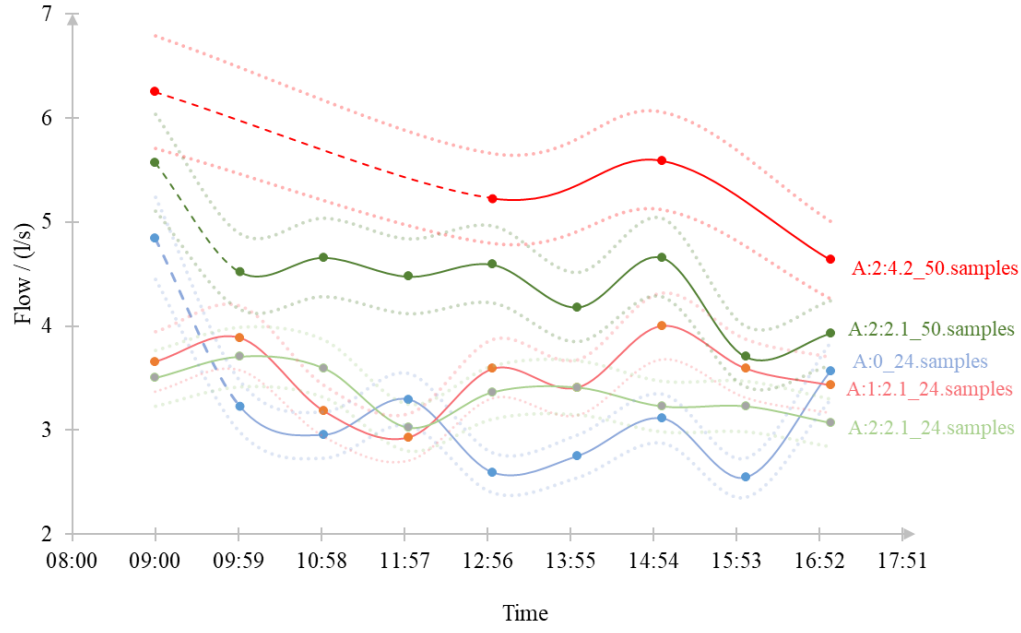

Figure 4.1b: The change in outgoing airflow with respect to time for different scenarios making use of inlet A. The dotted lines show the error margins of the flow measurements according to the standard given by Johansson and Svensson (1999). The dashed lines represent outlier data.

Figure 4.1a shows how the RH of the outgoing air changes as the drying period progresses. A downward trend is discerned for all experiments. As expected, the RH in the outgoing air for experiments containing 50 samples is higher than for experiments conducted on 24 samples. Figure 4.1b shows the change in the airflow exiting the drying chamber with regards to time. The dotted lines represent the error margins according to the standard

set by Johansson and Svensson (1999). Throughout the experiments the airflow varies insignificantly and the largest variation seen is of 1 l/s in scenario **A:1:2.1_24.samples**. Among the different scenarios the outgoing airflow varies, partly due to the external fan having different settings.

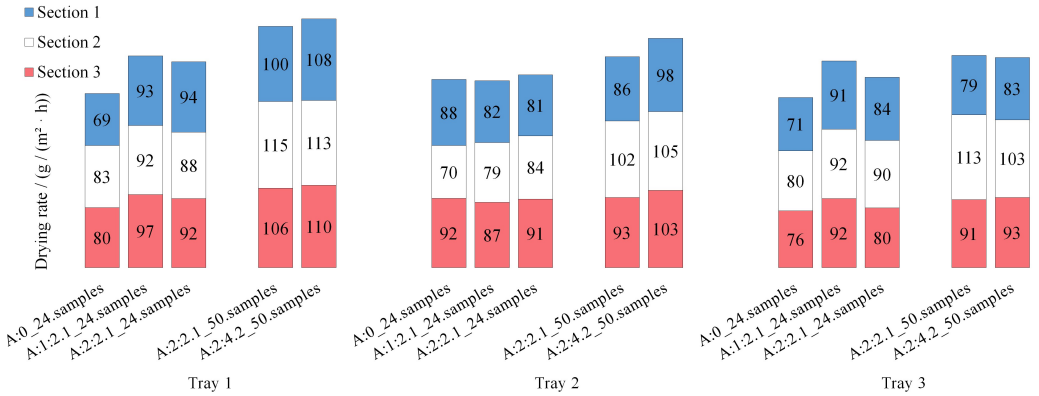

Figure 4.2a: The drying rate of the tray sections for different scenarios after approximately eight hours of drying.

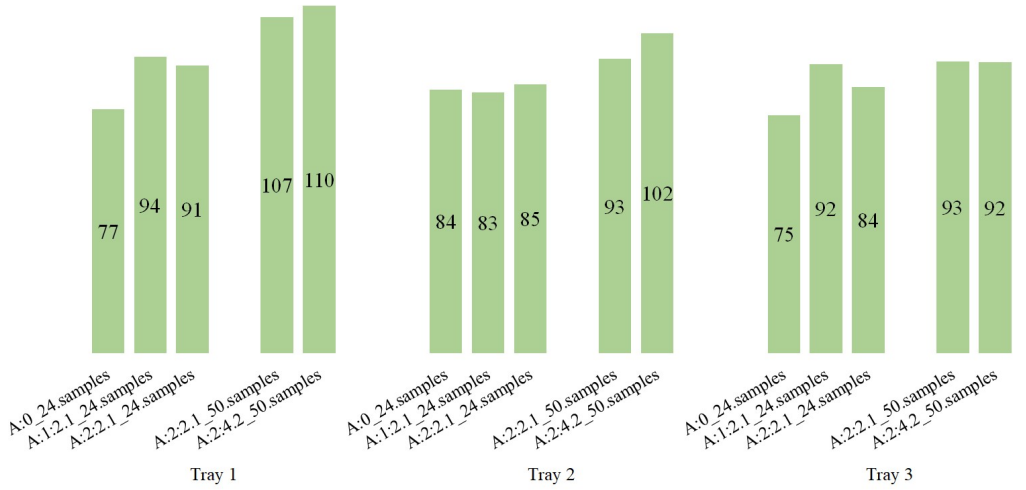

Figure 4.2b: The drying rate of the whole of tray 1 to tray 3 for different scenarios after approximately eight hours of drying.

Figure 4.2a shows the drying rate around eight hours post drying rounded to an integer for the different tray sections of tray 1, tray 2 and tray 3 as per equation 3.1. The aforementioned sections are described in appendix 7.3:figure 7.2. Figure 4.2b shows the drying rate after eight hours of drying for the whole of tray 1, tray 2 and tray 3 calculated as per equation 3.1.

Table 4.1: Table showing the percentage difference of the drying rate based on the previously mentioned scenario, the first reference scenario being: **A:0_24.samples**.

	A:1:2.1_24.samples / %	**A:2:2.1_24.samples / %**	**A:2:2.1_50.samples / %**	**A:2:4.2_50.samples / %**
Tray 1				
Section 1	34	1	6	8
Section 2	11	- 4	31	- 2
Section 3	22	- 6	15	4
Entire tray 1	**22**	**- 3**	**17**	**3**
Tray 2				
Section 1	- 7	- 1	6	14
Section 2	13	6	21	3
Section 3	- 5	5	2	10
Entire tray 2	**- 1**	**3**	**9**	**9**
Tray 3				
Section 1	28	- 8	- 6	5
Section 2	15	- 2	26	- 8
Section 3	22	- 14	14	3
Entire tray 3	**22**	**- 8**	**10**	**0**

Table 4.1 shows by how much the drying rate varies in comparison to the previously mentioned scenario. These values are calculated using the drying rate prior to rounding and is given in terms of percentage. For instance on the first tray with 24 samples there is a 11 % increase in drying rate on section 2 when going from no fan to one fan ($\frac{92}{83} \approx 1.11$). Adding a second fan decreases the drying rate by 4 % ($\frac{88}{92} \approx 0.96$). The procentual variation of the entire trays' drying rate in comparison to the previous scenario is also presented in table 4.1.

Comparison between the 24 samples experiments The drying rate of tray 1 and tray 3 shows a significant drying rate increase of 22 % between the case without any internal fan versus one fan. No significant increase between the use of one fan and two fans is discernible. Using two fans instead of one results in a drying rate decrease of 3 % for tray 1, an increase of 3 % for tray 2 and a decrease of 8 % for tray 3. When looking at entire trays for the case with no internal fans, tray 2 exhibits the highest drying rate. Adding one internal fan results in a higher drying rate for the trays located closest to and furthest from the inlet (tray 1 and tray 3, respectively). When two fans are added the drying rate decreases with the tray number. In other words, with two internal fans the tray closest to the inlet shows the highest drying rate while the tray furthest away from the inlet presents the lowest drying rate. The same pattern is expressed for the water activity (figure 4.4) which implies that the drying process is quicker for the tray located right above the internal fans, close to the inlet. The recirculation seem to be centred around tray 1 with a net flow up towards remaining trays.

Comparison between 24 samples versus 50 samples experiments with matching internal fan settings There is an increase in the drying rate for all trays of scenario **A:2:2.1_50.samples** when compared to scenario **A:2:2.1_24.samples**. As demonstrated

with the support of figure 2.1 and figure 4.4, a high drying rate in combination with elevated water activity indicate that a superior drying rate is simply due to the samples being at the beginning of their falling rate. A high drying rate is therefore not necessarily an indication of a faster drying process. It is observed that for both experiments conducted with 24 samples and with 50 samples tray 3, closely followed by tray 2, shows the lowest drying rate. As the air becomes saturated it is logical that the drying rate decreases with the raising number of trays.

Comparison between 50 samples experiments with different internal fan settings
Rising the voltage of the internal fans from 2.1 V to 4.2 V shows an increase in drying rate across the majority of sections and trays. The exception being for tray 3, where no change in the tray's drying rate is observed. Since the internal fans are placed low inside the drying chamber the air circulation is centred around tray 1, implying that despite a higher internal flow tray 3 is the least affected.

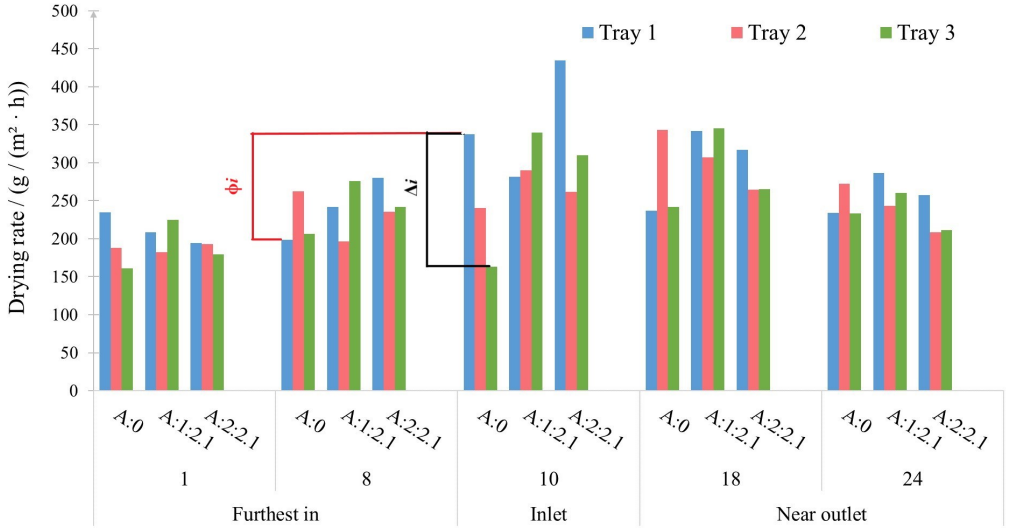

Figure 4.3: The integrated drying curves for the different points of interest after four hours of drying for the experiments conducted with 24 samples. The symbol ϕ_i and Δ_i are used to facilitate the explanation of table 4.2.

Figure 4.3 represents the integrated drying curves of the experiments conducted on 24 samples, four hours after drying, for the different points of interest shown in figure 3.7. This graph gives an indication on the evenness of the drying process. A similar value on the integrated drying rates between the different points of interest and between different trays indicates an uniform drying process. Two types of values are used to allow for a comparison to be made between the different scenarios. The first value looks at the drying evenness across the trays. This is calculated by taking the difference between the lowest and highest integrated drying rate per tray (see ϕ_i in figure 4.3). The second value aims to explain the uniformity of the drying process between trays. This value is calculated by taking the difference between the maximum and minimum integrated drying rate for each point of interest (see Δ_i in figure 4.3).

Once Δ_i for sample 1, 8, 10, 18 and 24 is extracted the average is calculated. The resulting values are rounded to the nearest integer and are seen in figure 4.2.

Table 4.2: Table showing values representing the uniformity of the drying process based on data from figure 4.3.

	A:0 / g / (h · m^2)	**A:1:2.1** / g / (h · m^2)	**A:2:2.1** / g / (h · m^2)
Across trays			
Tray 1	139	133	241
Tray 2	156	125	71
Tray 3	81	120	130
Between trays	92	52	67

Table 4.2 depicts that scenario **A:1:2.1** gives the most uniform drying process between the trays with an average difference between samples of 52 g / (h · m^2). The most uneven drying process between trays is given when no fans are used and is of 92 g / (h · m^2). When looking at how uniform the drying process is across trays, tray 1 making use of one fan exhibits the most even drying process. This is to be expected as the internal fans are placed below tray 1. When looking at tray 2, this title is awarded to the scenario with two fans. For tray 3, the most uniform drying process across the tray is expressed when no fan is used. However, using one fan gives the second most uniform drying process for both tray 2 and tray 3.

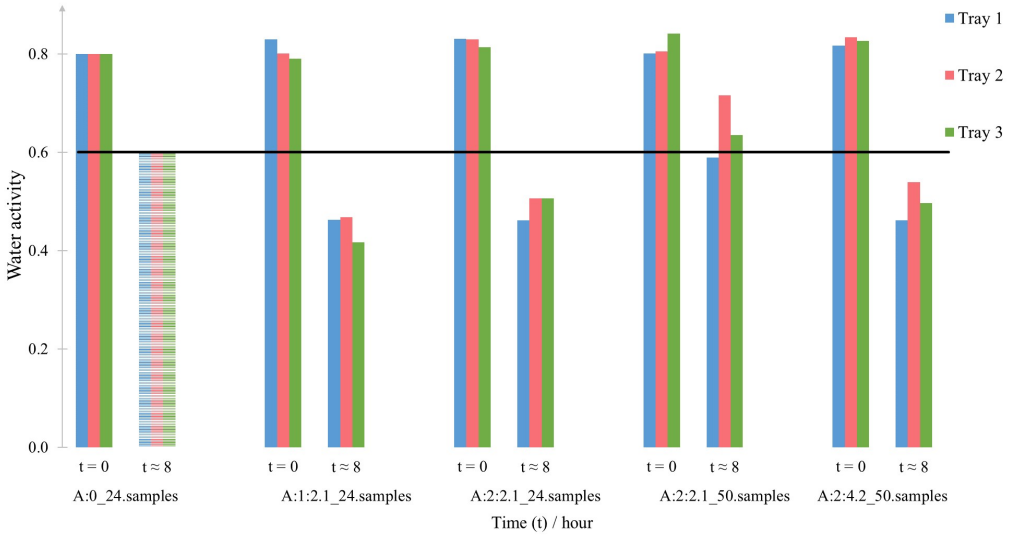

Figure 4.4: Water activity levels before drying and approximately eight hours post drying for different scenarios. The stripped bars represent unassertive data. The horizontal black line indicates the limit at which the samples are deemed dried enough to prohibit microbial growth. *t* refers to the amount of time the products are dried for, given in the unit of hour.

Figure 4.4 describes the trays' water activity level for different experiments prior to drying (t = 0) and around eight hours post drying (t ≈ 8). The striped bars of

A:0_24.samples represent lack of retrieved data due to damaged files. However, the available measurements show a water activity below 0.6. The horizontal black line in figure 4.4 indicates the limit at which the samples are considered dried enough to prohibit microbial growth. As shown in figure 4.4 all experiments yield a water activity level below the acceptable limit of 0.6, except for tray 2 and tray 3 of scenario **A:2:2.1_50.samples**. Increasing the internal airflow through a rise in the fans voltage from 2.1 V to 4.2 V allows for scenario **A:2_50.samples** to reach the required water activity level. The other scenarios (**A:1:2.1_24.samples** and **A:1:2.1_24.samples**) exhibit a water activity of at least 15 % below the set requirement of 0.6 and at most $\approx$ 31 % below the required value.

4.2 Setup using inlet B: scenarios using the top inlet

When using the top inlet the challenge lays in forcing the warm air down into the chamber. To ensure that this is possible the internal fan is set to its highest voltage (12 V). If the air is not compelled to move down into the chamber while the highest fan setting is used, then all experiments using the top inlet are considered unnecessary. Once it is proven that the warm air is able to move down into the chamber and the optimum fan number is found, the voltage of the internal fans are reduced to help find their lowest optimal airflow. To accommodate the fan, tray 2 is removed from the experiments using two fans. This is the reason for the missing values of tray 2 for scenarios **B:2:12_24.samples**, **B:2:9_50.samples** and **B:2:12_50.samples**. Another important detail to highlight is that scenario **B:2:12_24.samples**' drying period is of five instead of eight hours.

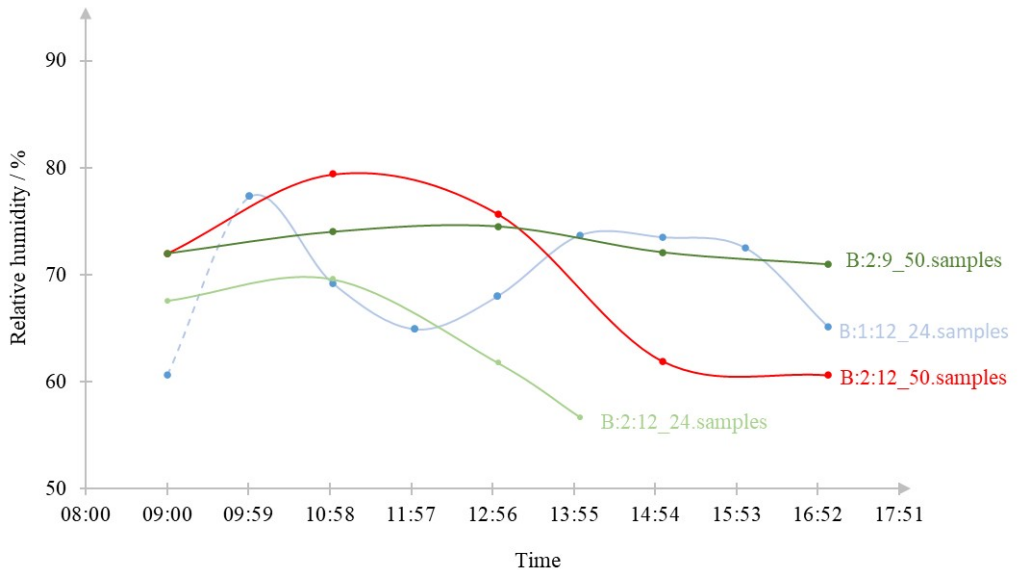

Figure 4.5a: The change of RH humidity in the outgoing air with respect to time for different scenarios making use of inlet B. The dashed lines represent outlier data.

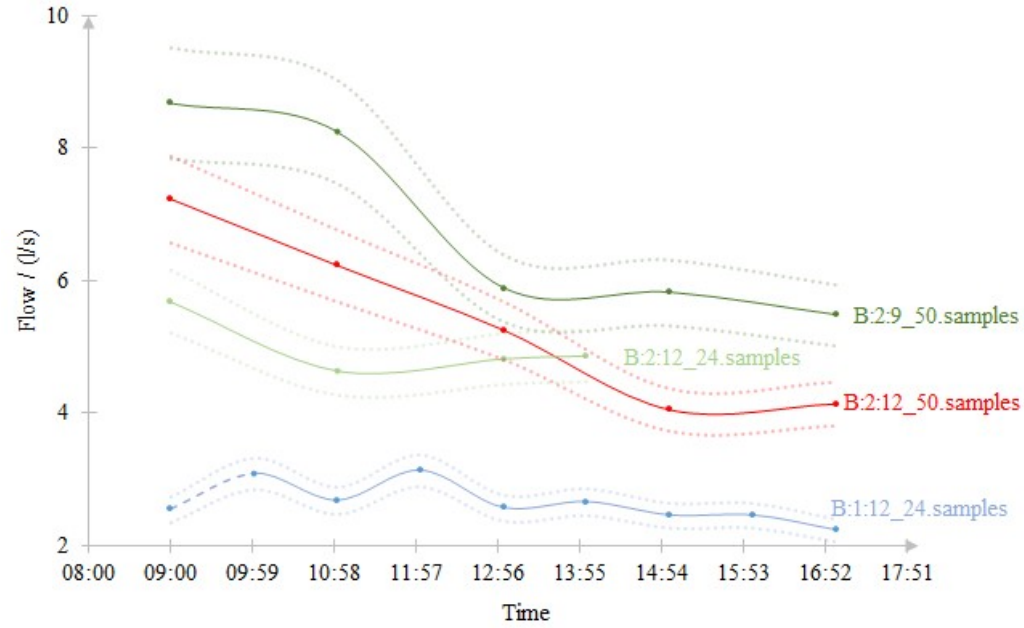

Figure 4.5b: The change in outgoing airflow with respect to time for different scenarios making use of inlet B. The dotted lines show the error margins of the flow measurements according to the standard given by Johansson and Svensson (1999). The dashed lines represent outlier data.

The indoor conditions of the drying period for different experiments is seen in figure 4.5. Figure 4.5a illustrates a decrease in the outgoing air's RH of around 12 percentage points for scenario **B:1:12_24.samples**. A decrease in RH of approximately 11 percentage point is observed for scenario **B:2:12_50.samples** and scenario

B:2:12_24.samples. All the while, the RH decreases with 1 percentage point for scenario **B:2:9_50.samples**. Figure 4.5b shows the variation in the airflow out of the drying chamber throughout the drying period. The dotted lines represent the error margins according to the standard set by Johansson and Svensson (1999). The flow varies with approximately 3 l/s for both scenario **B:2:9_50.samples** and scenario **B:2:12_50.samples**. The flow variation for **B:2:9_50.samples** is attributed to the internal fan's setting being changed from 12 V to 9 V after four hours of drying, due to to a preparation mistake. The noticeable flow variation in scenario **B:2:12_50.samples** is assigned to the measurement plan falling close to invalid, according to the standard set by Johansson and Svensson (1999). The standard requires the maximum velocity to be $\leq 1.4 \cdot$ centre velocity. This requirement is only 7 % away from not being fulfilled, while for the other scenarios the measurement plan falls amply within the required limits (with at least a margin of 17 %). For scenario **B:1:12_24.samples** and scenario **B:2:12_24.samples** the airflow manifests an insignificant flow variation of maximum 1 l/s throughout the experiment. Lastly, it is observed that varying the number of internal fans inside the drying chamber does affect the outgoing airflow. Figure 4.5b shows a lower outgoing airflow when only one internal fan is used in comparison to two internal fans.

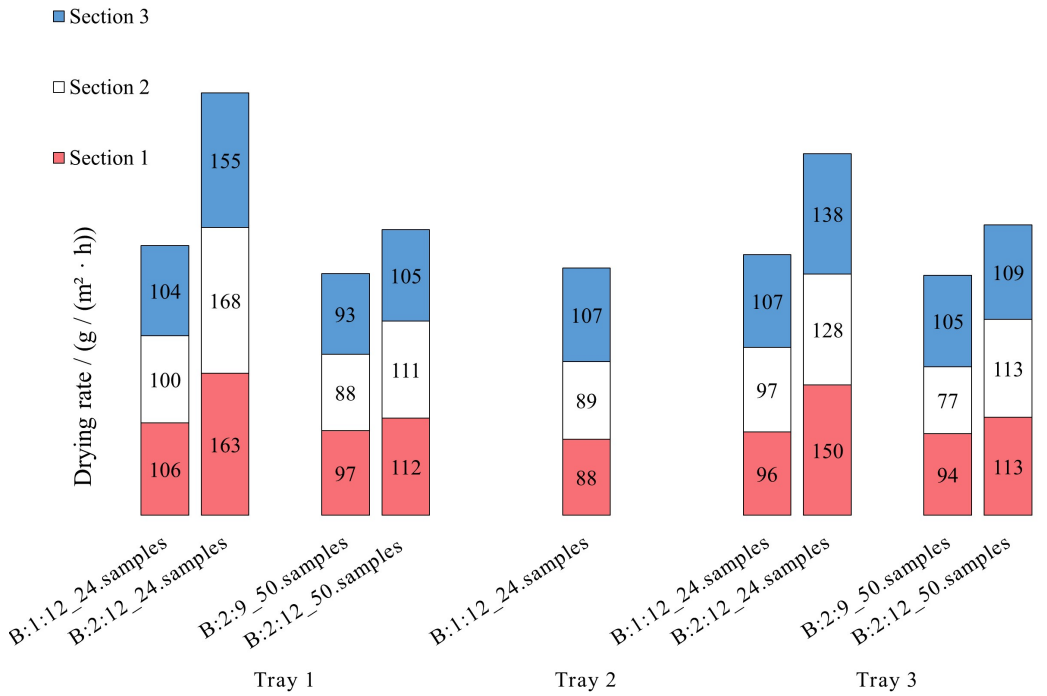

Figure 4.6a: The drying rate of the tray sections for different scenarios after completed experiment.

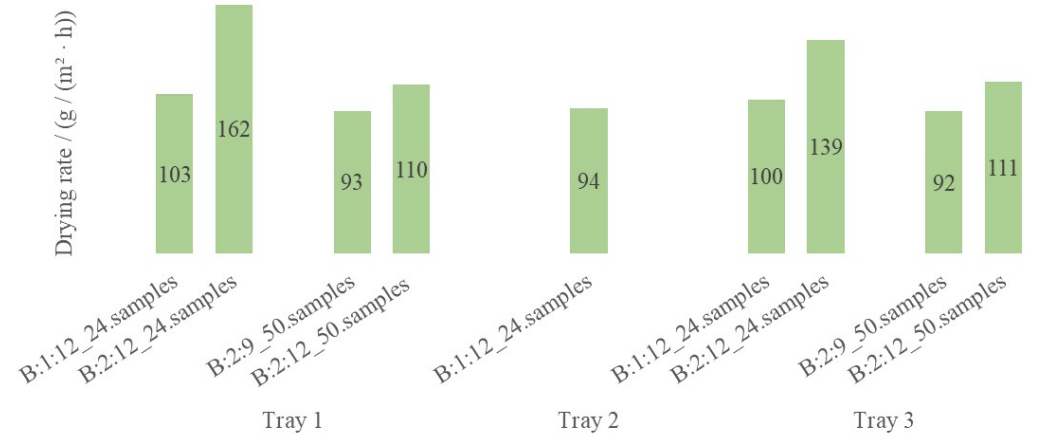

Figure 4.6b: The drying rate of the whole of tray 1 to tray 3 for different scenarios after completed experiment.

Figure 4.6a shows the drying rate post drying rounded to an integer of the different tray sections for all the trays as per equation 3.1. The aforementioned sections are described in appendix 7.3:figure 7.2a and figure 7.2b. Figure 4.6b shows the drying rate for the whole of tray 1, tray 2 and tray 3 for different scenarios calculated as per equation 3.1.

Table 4.3: Table showing the percentage difference of the drying rate based on the previously mentioned scenario, the first reference scenario being: **B:1:12_24.samples**.

	B:2:12_24.samples / %	**B:2:9_50.samples / %**	**B:2:12_50.samples / %**
Tray 1			
Section 1	53	- 40	15
Section 2	68	- 48	27
Section 3	49	- 40	14
Entire tray 1	**57**	**- 43**	**18**
Tray 2			
Section 1	-	-	-
Section 2	-	-	-
Section 3	-	-	-
Tray 3			
Section 1	56	- 37	20
Section 2	32	- 40	47
Section 3	29	- 24	3
Entire tray 3	**39**	**- 33**	**21**

Table 4.3 indicates by how much the drying rate varies in comparison to the previously mentioned scenario. These are calculated using the drying rate values prior to rounding and is given in terms of percentage. The procentual variation of the entire trays' drying rate in comparison to the previous scenario is also presented in table 4.3.

Comparison between the 24 samples experiments Using two fans results in a drying rate increase of 57 % for tray 1 and 39 % for tray 3 in comparison to when only one fan is used. For both scenarios, the tray furthest away form the inlet (tray 1) shows a higher drying rate than the tray closest to the inlet (tray 3). According to figure 4.8 the water activity is higher for the tray further away from the inlet, even though its drying rate is superior. This indicates once more that a high drying rate can symbolise a less progressed drying process and is not necessarily a sign of good heat transfer.

Comparison between the 24 versus 50 samples experiments with matching internal fan settings Fully loading the drying chamber decreases the drying rate across all sections and all trays. The drying rate of tray 1 decreases with approximately 30 % when looking at scenario **B:2:12_24.samples** versus scenario **B:2:12_50.samples**. When examining tray 3, it is seen that the tray's drying rate decreases with approximately 20 %. For the 24 samples experiment the tray furthest away from the inlet (tray 1) presents a higher drying rate than the tray closest to the inlet (tray 3). For the 50 samples experiment the drying rate between the trays is similar.

Comparison between 50 samples experiments with different internal fan settings As indicated in table 4.3, turning up the internal fans' airflow results in a positive increase of the drying rate. The increase for tray 1 is 18 % and respective value for tray 3 is 21 %. The maximum increase in drying rate for both tray 1, as well as tray 3, is seen in section

2 and is 27 % and 47 %, respectively.

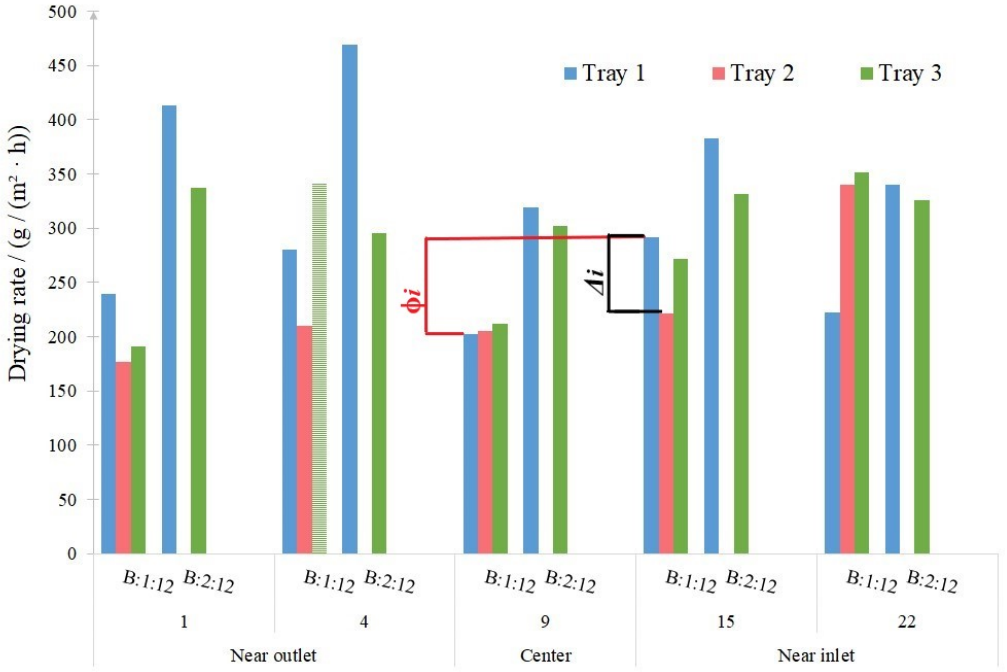

Figure 4.7: The integrated drying curves for the different points of interest after four hours of drying for the experiments conducted with 24 samples. The striped bars represent outlier data as a result of the measurements being made on the wrong sample piece. The symbol ϕ_i and Δ_i's are used to facilitate the explanation of table 4.4.

Figure 4.7 represents the integrated drying curves of the experiments conducted on 24 samples, four hours after drying, for the different points of interest shown in figure 3.7. This graph gives an indication on the evenness of the drying process. To simplify the presented data two types of values are used, as previously explained in chapter 4.1. The first value looks at the drying evenness across the trays (see ϕ_i in figure 4.7) while the second value aims to explain the uniformity of the drying process between trays (see Δ_i in figure 4.7). The resulting values are rounded to the nearest integer and are seen in figure 4.4.

Table 4.4: Table showing values representing the uniformity of the drying process based on data from figure 4.7.

	B:1:12 / g / (h · m^2)	**B:2:12** / g / (h · m^2)
Across trays		
Tray 1	90	150
Tray 2	163	-
Tray 3	161	41
Between trays	69*	66

*The collected data for sample piece 4 of tray 3 is not valid and therefore not taken into consideration when preforming the calculations.

As indicated with table 4.4, two fans result in a more uniform drying process across the trays than one fan. The average integrated drying rate difference between the trays is of 66 g / (h · m^2) and 69 g / (h · m^2), respectively. When analysing tray 1's drying uniformity it is seen that the smallest difference in drying rate between samples is while using one fan (90 g / (h · m^2)). Hence, for tray 1, the drying process is more uniform when using one fan instead of two. When looking simultaneously at scenario **B:1:12** and scenario **B:2:12** the most even drying process across trays is seen for the tray closest to the inlet (tray 3), when two fans are used. It should be noted that the maximum integrated drying rate difference between points of interest when using two internal fans (150 g / (h · m^2)) is lower than that of tray 2 and tray 3 of the scenario using one internal fan (163 g / (h · m^2) and 161 g / (h · m^2), respectively).

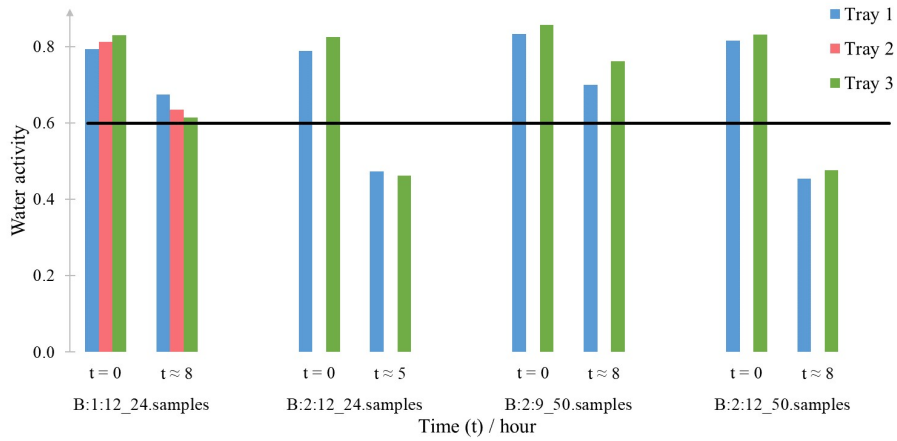

Figure 4.8: Water activity levels before and after drying for different scenarios. The horizontal black line indicates the limit at which the samples are deemed dried enough to prohibit microbial growth. *t* refers to the amount of time the products are dried for, given in the unit of hour.

Figure 4.8 describes the trays' water activity level for different experiments prior to and post drying. The horizontal black line in figure 4.8 shows the limit at which the samples are considered dried enough to prohibit microbial growth. As seen in figure 4.8 the

required water activity level is reached for all scenarios, except for scenario **B:1:12_24.samples** and **B:2:9_50.samples**. For **B:2:12_24.samples** the desired level is obtained after approximately 5 hours of drying. Scenarios **B:2:12_24.samples** and **B:2:12_50.samples** exhibit a water activity level of at least 20 % below the required limit.

4.3 Comparison between setup using inlet A and setup using inlet B

This chapter contains figures that are relevant to the discussion conducted in chapter 5 and is therefore not addressed until relevant chapter. The figures represent the drying rate of the trays' sections (figure 4.9) and the water activity prior to as well as post drying (figure 4.10) for scenario **A:1:2.1_24.sample** and scenario **B:2:12_24.sample**. Figures showing the inside temperature of the dryer deemed relevant to the discussion are presented. These figures are shown to make it easier to follow the discussion in chapter 5 and to help illustrate the results in a clearer and simpler way.

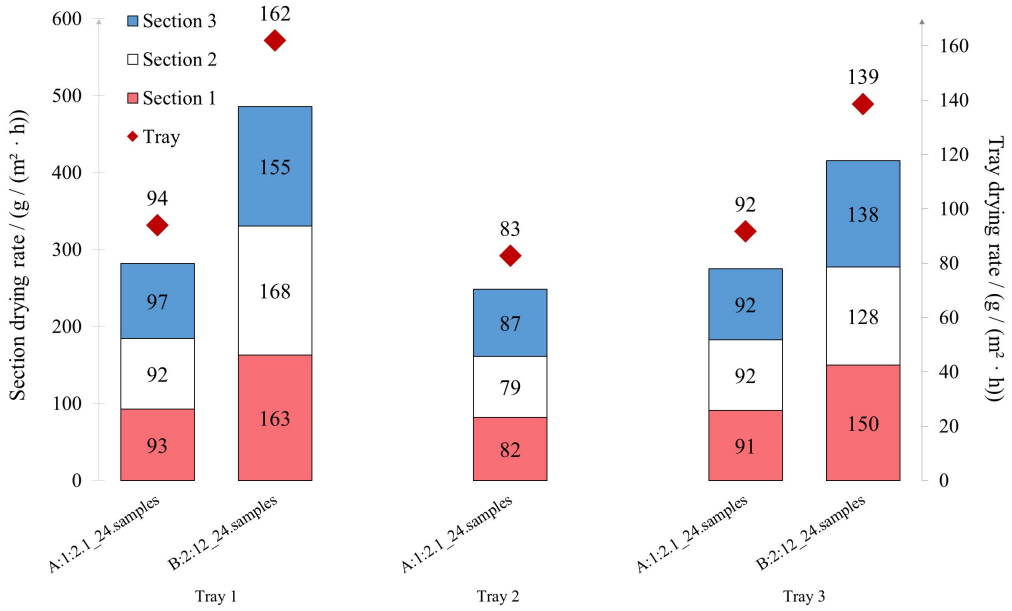

Figure 4.9: The drying rate of the tray and the tray's sections for scenario **A:1:2.1_24.sample** and scenario **B:2:12_24.sample** after completed experiment.

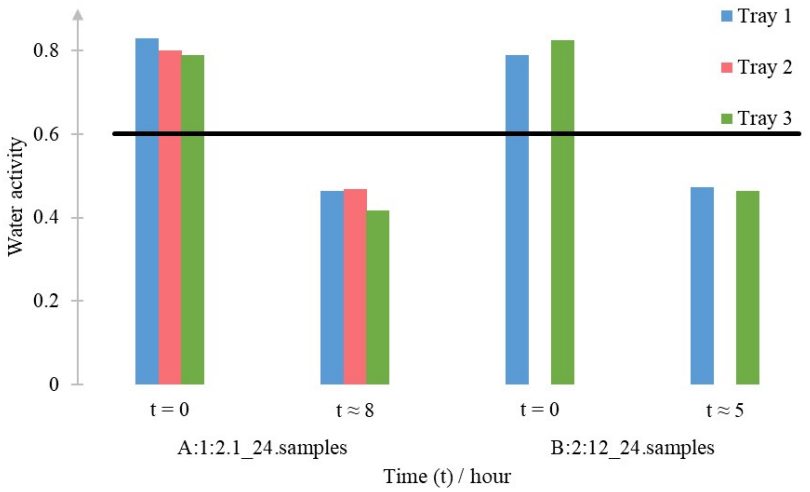

Figure 4.10: Water activity levels before and after drying for scenario **A:1:2.1_24.sample** and scenario **B:2:12_24.sample**. The horizontal black line indicates the limit at which the samples are deemed dried enough to prohibit microbial growth. *t* refers to the amount of time the products are dried for, given in the unit of hour.

4.3.1 Temperature

Figure 4.11 shows the inside temperature for scenarios **A:1:2.1_24.samples**, **A:2:2.1_24.samples**, **B:2:12_24.samples** and **B:2:12_50.samples**. The dryer's sides are named according to figure 3.5. Values that differ with more than 2 °C from at least one of their enclosing value are considered to be outliers and are excluded from the data. These outliers are attributed to the malfunctioning of the thermocouples. Lack of data due to the thermocouples' inability to produce values are also seen as outliers and removed. Furthermore, the cooling and reheating periods due to the opening of the dryer are eliminated from the data. To simplify the comparison between scenarios, the average temperature of the trays is calculated for each of the dryer's side. The time at which the experiments are started is not a parameter that affects the outcome, therefore the same initial time has been selected for all experiments when presenting the result. This choice is made to enable clearer data presentation and to help simplify comparison. The dotted red lines in figure 4.11 represent the moment at which the trays are put in the dryer. When the trays are inserted it can be seen that the chamber cools to different levels, resulting in varying starting temperatures for the experiments. Since the initial temperature varies it makes a comparison of the dryer's temperature between different scenarios impossible.

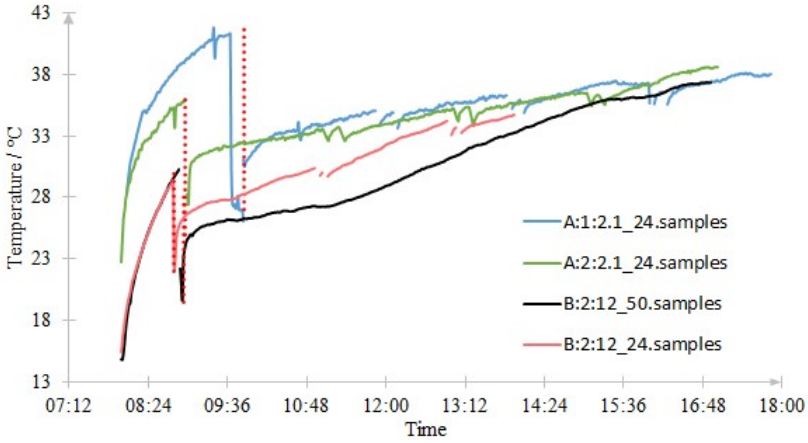

Figure 4.11a: The average of the drying chamber's internal temperature of side lgO for scenarios **A:1:2.1_24.samples**, **A:2:2.1_24.samples**, **B:2:12_24.samples** and **B:2:12_50.samples**. The dotted red lines indicate the moment the trays are inserted.

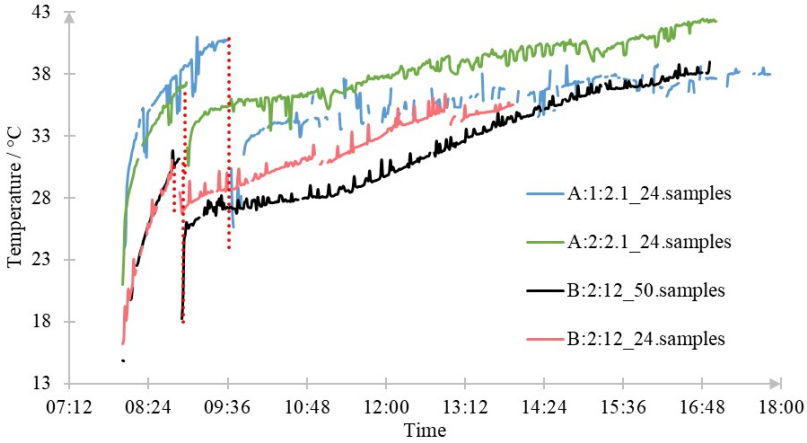

Figure 4.11b: The average of the drying chamber's internal temperature of side lgH for scenarios **A:1:2.1_24.samples**, **A:2:2.1_24.samples**, **B:2:12_24.samples** and **B:2:12_50.samples**. The dotted red lines indicate the moment the trays are inserted.

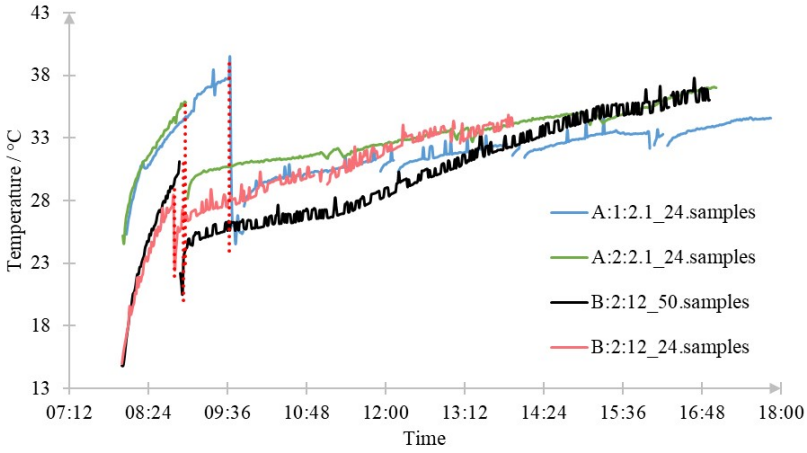

Figure 4.11c: The average of the drying chamber's internal temperature of side shB for scenarios **A:1:2.1_24.samples**, **A:2:2.1_24.samples**, **B:2:12_24.samples** and **B:2:12_50.samples**. The dotted red lines indicate the moment the trays are inserted.

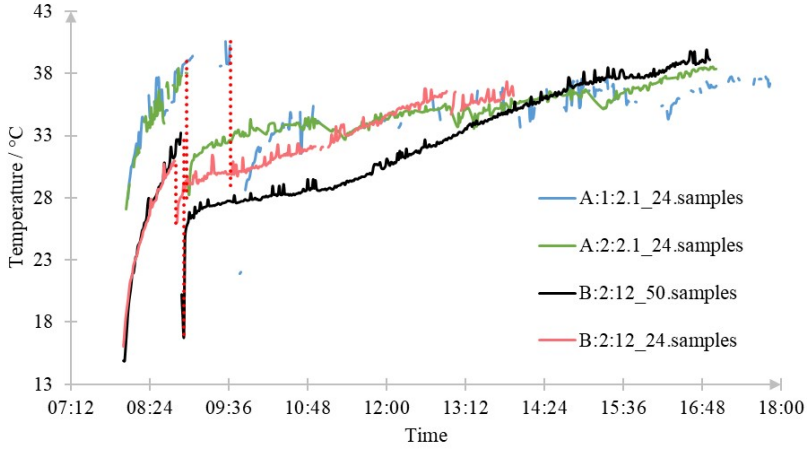

Figure 4.11d: The average of the drying chamber's internal temperature of side shD for scenarios **A:1:2.1_24.samples**, **A:2:2.1_24.samples**, **B:2:12_24.samples** and **B:2:12_50.samples**. The dotted red lines indicate the moment the trays are inserted.

The temperature prior to inserting the drying trays for scenarios **A:1:2.1_24.samples** and scenario **A:2:2.1_24.samples** is higher than the other two scenarios. The reason being that the heat lamps are started shortly before the first measurements are taken while for the remaining two scenarios, the temperature is measured before the heat lamps are turned on. It is observed that for all sides of scenario **A:1:2.1_24.samples** and scenario **A:2:2.1_24.samples**, the temperature at which the trays are placed inside the drying chamber varies with a maximum of 3 °C. As seen in figure 4.11, the temperature stays within the same range throughout the drying process for sides lgO, shB and shD of the scenarios using inlet A.

When comparing scenario **B:2:12_24.samples** with **B:2:12_50.samples**, is is observed that **B:2:12_24.samples** has a higher temperature during the drying process. The

starting temperature at which the trays are introduced into the dryer differs between the two scenario with at its most 7 °C. The higher internal temperature can not be explained by the increase in samples as their starting conditions differ.

The temperature at which the trays are inserted varies with a maximum of 3 °C between scenario **A:1:2.1_24.samples** and **A:2:2.1_24.samples**, a maximum of 16 °C between scenario **A:2:2.1_24.samples** and **B:2:12_24.samples** and a maximum of 7 °C between scenario **B:2:12_24.samples** and **B:2:12_50.samples**. Hence, nothing can be said about how the different inlets and scenarios influence the temperature.

5 Discussion

This work aims to enhance the heat transfer and create an even drying process inside a drying chamber by focusing on the internal airflow. Two inlets are tested to find the optimal placement together with the required number of fans to create a fast and uniform drying process. The impact of varying the airflow of the internal fans and their placement is also discussed. However, prior to discussing which of the inlets yield the best result, it should be noted that the method used to record the drying rate has some flaws.

An issue with recording the samples' change in weight instead of their water activity throughout the drying period is that the drying rate can easily be misinterpreted. A high and constant drying rate is to be favoured throughout the drying period, however, like figure 2.1 shows there is a falling rate. The falling rate is expressed as a low drying rate value. Hence, if the drying rate is low while the samples exhibits a low water activity level, it can imply that there is good heat transfer taking place and the samples are simply further along the drying curve. Therefore, integrating the drying rate after four hours, when the samples are not fully dried, gives a clearer indication on how effective the drying process is (figure 4.3 and figure 4.7).

Temperature is another important factor to note before using the drying rate as a measure of how good the heat transfer is in the drying chamber. If the temperature is high, the increase in heat transfer can be due to the temperature and not because of induced airflow inside the drying chamber. On the other hand, a lower temperature does not necessarily mean an inferior drying process. On the contrary, it can be an indication of an intense drying process as the evaporation of water is an endothermic reaction. A lower temperature can also be an indication that the warm air is better mixed, resulting in a lower but more uniform temperature across the chamber. Before drawing any conclusions the drying rate, water activity and temperature should be taken into account.

5.1 Optimal scenario making use of inlet A

Figure 4.2b shows that the use of one internal fan compared to no fan increases the average drying rate significantly, with some exception for tray 2, which exhibits a decrease of 1 %. Adding a second fan leads to an overall decrease in drying rate. As previously mentioned,

a lower drying rate does not necessarily indicate an inferior drying process. When looking at figure 4.4, scenario **A:1:2.1_24.samples** shows a lower water activity level together with a higher drying rate in comparison to scenario **A:2:2.1_24.samples**. This can be interpreted as using one internal fan gives a higher drying rate throughout the entire drying process compared to when two internal fans are used. However, this interpretation is not valid at all times since there is a possibility that the result looks different if the fans for each scenario are moved around.

It is known that the increased drying rate is not due to a difference in temperature between the scenarios, since for three of the dryer's sides the temperature lays within the same range (figure 4.11). This is true indifferent of the number of internal fans used. The temperature is slightly higher for one of the long sides when two internal fans are active (figure 4.11a). Figure 4.10 shows that using one fan results in inferior water activity levels for all trays even if the temperature is lower than when two fans are used.

Using one fan gives the most even drying process between trays and indicates a second to best drying uniformity across the trays (table 4.2). The average integrated drying rate difference between trays is of approximately 92 g / ($h \cdot m^2$) when no internal fans is present, 52 g / ($h \cdot m^2$) when one fan is used and approximately 67 g / ($h \cdot m^2$) when two fans are active. In conclusion, scenario **A:1:2.1** gives the most uniform drying process between trays and the second most even drying process across the trays.

When loading the dryer with 50 samples, figure 4.4 shows that two fans are not enough to reach a water activity level which prohibits microbial growth. This is anticipated since a loaded chamber saturates the dryer's air with moisture faster than when only 24 samples are dried. Nevertheless, increasing the internal fans' setting to 4.2 V allows for the desired water activity level to be reached. Increasing the internal airflow inside the chamber by rising the fans' voltage results in better convection, which is noticed in the form of a higher drying rate for the majority of the trays. Hence, a higher internal airflow leads to better heat transfer and results in the samples reaching a desired water activity level.

It should be said that if the iterative process seen in figure 3.8 is followed correctly, the fans' airflow should have been varied for the scenario utilising one fan, not two fans. This was not discovered until later when the data analysis was completed and time was running out. In other words, experiments on a loaded chamber with 50 pieces, using one internal fan set to 2.1 V and 4.2 V, should have been conducted. Since scenarios **A:1:2.1_50.samples** and **A:1:4.2_50.samples** were not tested there is a possibility of another, more advantageous, local optimum being present but not identified.

Based on the experiments done for the setup using inlet A, one fan with a voltage of at least 4.2 V seems to be the best alternative. This, as it yields the highest drying rate as well as an uniform drying process.

5.2 Optimal scenario making use of inlet B

Table 4.3 indicates that using two fans instead of one increases the drying rate for tray 1 and tray 3 with 57 % and 39 %, respectively. It is possible that this increase is a result of the presence of fewer samples inside the dryer, since two trays instead of three are used. The required water activity level is not reached with one fan set to 12 V with an initial chamber load of approximately 520 gram, spread out as 24 samples on three trays. It is however reached for the scenario using two fans set to 12 V with an initial chamber load of approximately 800 gram, spread out as 50 samples on two trays. Therefore the speculation that a higher drying rate is obtained when two fans are used due to a lesser load in the drying chamber is eliminated.

Regarding the drying uniformity, utilising two fans instead of one helps increase the evenness of the drying process between the drying trays. The maximum integrated drying rate difference between points of interest when using two internal fans is lower (150 g / ($h \cdot m^2$)) than that of tray 2 and tray 3 of the scenario using one internal fan (163 g / ($h \cdot m^2$) and 161 g / ($h \cdot m^2$), respectively). The use of two internal fans is therefore presumed to give a satisfactory drying process across the trays.

When two internal fans set to 12 V are in place and the drying chamber is loaded with 50 samples instead of 24 samples, there is a decrease in the drying rate. Despite this, the water activity level requirement is fulfilled for both cases. When fully loading the dryer and decreasing the two internal fan's setting from 12 V to 9 V, the drying rate decreases with approximately 20 % for both trays (figure 4.6a) and the desired level of water activity is not reached. Considering that the temperature at which the apples are dried is higher when conducting the experiment on 24 samples, it can not be dismissed that the higher drying rate between these two scenarios is because of the temperature (figure 4.11).

When using inlet B, utilising two fans with a voltage of 12 V seems to be the best alternative for the uniformity of the drying process as well as from a heat transfer perspective. It is known that the optimal internal fans' airflow which gives a high drying rate, an uniform drying process, while utilising a minimum amount of energy lays between a fan setting of 9 V to 12 V.

5.3 Optimal design

A comparison between the optimal scenario of inlet A and inlet B can only be made between the experiments conducted on 24 samples. This since the optimal scenario of inlet A is not tested for a fully loaded chamber, due to lack of time.

When looking at the optimal design from a heat transfer perspective, figure 4.9 indicates that the drying rate is higher for scenario **B:2:12_24.sample** than for scenario **A:1:2.1_24.samples**. As previously mentioned, a high drying rate does not necessarily imply a quicker drying process but can be an indication that the apple slices have not dried long enough to reach the falling rate (figure 2.1). This is a probable explanation of

the high drying rate exhibited for scenario **B:2:12_24.sample**, as the samples have dried three hours shorter than for scenario **A:1:2.1_24.samples**.

The water activity level is, for tray 1 and tray 2 of **B:2:12_24.samples**, approximately 2 % and 10 % higher, respectively (figure 4.10). The reason for the higher water activity for the scenario using inlet B is attributed to its shorter drying time. Since the water inside the samples do not evaporate linearly, there is the possibility that the water activity at $t \approx 5$ for inlet A is the same as for inlet B. The difference in water activity level between the scenarios is deemed small enough to be presumed similar. Hence, the high drying rate seen for scenario **B:2:12_24.samples** can be an indication of the chamber's superior heat transfer.

In summary, it can be said that scenario **B:2:12_24.sample** has a higher drying rate, implying better heat transfer than scenario **A:1:2.1_24.samples**. Moreover, figure 4.11a and figure 4.11b show that for the two long sides of scenario **A:1:2.1_24.samples**, the temperate is higher throughout the drying process than that of **B:2:12_24.samples**. The short sides display similar temperature range throughout the drying process (figure 4.11c and figure 4.11d). It is therefore speculated that one possible explanation for the higher drying rate in scenario **B:2:12_24.samples** is due to the internal airflow and not because of a higher temperature inside the dryer.

When looking at the uniformity of the drying process between trays, scenario **B:1:12_24.samples** shows an average integrated drying rate difference of 66 g / ($h \cdot m^2$). Corresponding value for scenario **A:1:2.1_24.samples** is 53 g / ($h \cdot m^2$). This indicates that inlet A gives a more uniform drying process between the different trays. When looking at the drying uniformity across trays, the most even drying process is found for the tray nearest the inlet for the setup using inlet B (tray 3). For tray 3, the largest integrated drying rate difference between the points of interest is 41 g / ($h \cdot m^2$). The least uniform drying process between the two optimum scenarios is found for the tray furthest away from the inlet of the setup using inlet B (tray 1), it is expressed as a difference of 150 g / ($h \cdot m^2$). Using inlet A indicates a more even drying process for all three trays (133 g / ($h \cdot m^2$), 125 g / ($h \cdot m^2$) and 120 g / ($h \cdot m^2$)), when compared to the least uniform drying process (150 g / ($h \cdot m^2$)). In summary, using inlet A seems to result in a more even drying process between trays and a satisfactory drying uniformity across the trays.

The optimal design that gives the best heat transfer and most even drying process when the drying chamber is fully loaded can not be decided. This since scenario **A:1:2.1_50.samples** was not tested. Although, it seems that scenario **B:2:12_24.sample** gives a better heat transfer while scenario **A:1:2.1_24.samples** seems to have a more uniform drying process.

Before choosing which scenario is most efficient, the implications that each scenario has on the design of the dryer needs to be discussed and a compromised needs to be made between the uniformity of the drying process and the drying time. If looking at the

intended design of the solar dryer (figure 3.2), then using inlet B has some advantages. The first being that inlet B gives a less complex design since the entire back panel leading the air down and into the chamber can be removed. Hence, the air can directly be lead into the drying chamber once heated up by the absorber, reducing heat losses outwards. A disadvantage of using inlet B is that the design becomes dependent on the internal fans to function. However, if inlet A is used and the internal fans break down then natural convection will take over and the dryer will still work, albeit less efficiently. The possibility of adding a heat storage is available for both inlets. If the bottom inlet is used the heat storage can be placed above the inlet, at the bottom of the dryer. If the top inlet is used then the extra space under the absorber can be used as heat storage. One of the benefits of placing the heat storage under the absorber is that the space of the drying chamber is not reduced. A downside with using inlet B is that the trays must be redesigned to accommodate the fans. This can be solved by an increase of the space between the trays or a decrease of their widths.

In summary, if the heat transfer capacity and drying time is considered more important, then the solar dryer's chamber should be designed based on scenario **B:2:12_24.sample**. If the uniformity of the drying process is more important then scenario **A:1:2.1_24.samples** is the best choice. Using inlet A has the advantage of ensuring that even if the internal fans break the dryer still functions adequately. However, it has the disadvantage that if a heat storage is added the space used for drying nutriments decreases. Using inlet B makes the solar dryer's design less complex, but makes it dependent on the internal fans functioning. Using the top inlet also has the advantage that a heat storage can be installed without diminish the drying chamber's area.

5.4 Fan placement

The initial placement of the first fan for the setup using inlet A (figure 3.9) is selected based on where the temperature is the lowest in the scenario using no fans. The goal being to relocate warm air into that area. The second fan is placed with the intent of ensuring that all trays have a uniform drying process. It is therefore placed where the lowest drying rate is seen when one internal fan is used, which is near section 1 (figure 4.2a). Different placements for the fans should be tested to find the optimal drying conditions and if possible, reduce the dryer's complexity by decreasing the number of fans used. The optimal scenario found is **A:1:2.1** which implies that moving the fan around can only lead to increase in drying rate and drying uniformity, but not to a reduction in the design's complexity. It is found that with two fans the drying rate decreases whilst the water activity level increases. Hence, different placements of the fans can lead to an increase in the drying rate, however, this is only favourable if it surpasses the result of the current optimal scenario, **A:1:2.1**.

The first fan in the setup using inlet B is placed with the intention of enabling the incoming air to be pulled down into the chamber (figure 3.9). The second fan is placed based on where the temperature is the lowest in the scenario using one fan. This since a low

temperature indicates that the warm air does not reach that specific area. The fan below the inlet is essential to achieve an even drying process and good heat transfer, it can therefore not be relocated. Moving the second fan is unnecessary as the only potential other placement is either to switch it to the other long side or change its angle. Both these options are considered too small to reverberate significant changes in the results.

5.5 Potential method improvement

To improve the experiments the first thing to do is to relocate the bottom inlet. The bottom inlet can be moved from the centre of the chamber to as far away as possible from the outlet. The reason being that for the scenario with no fan, the warm air can potentially cover a larger area of the drying chamber before exiting the dryer. This can lead to a higher drying rate which would resonate throughout all experiments. Another improvement to be done is to shorten the time of the experiments. As seen in figure 4.4 and figure 4.8, the water activity level falls below the required limit for some scenarios. This indicates that the samples are considered dried before the experiments end. Time can be spared by shortening the experiments.

Another method flaw is the way the drying rate is calculated since using the initial active surface area underestimates the drying rate. According to an experiment conducted by Subedi et al. (2019) the shrinkage of sliced apple cubes is not isometric. During convective drying of approximately four to five hours, the apple slices' diameter shrink with about 14 % to 20 % compared to raw apples (Subedi et al., 2019). All the while Subedi et al. (2019) write that the height decreases with about 34% at 50 °C. It is assumed that this error margin occurs across all conducted experiments. Hence, the drying rates are still relevant and valid to use as comparative results between the experiments. This issue can be eliminated by measuring the water activity of the points of interest throughout the experiment instead of the mass. Furthermore, measuring the water activity for each tray sections at the end of the experiments can help give a clearer indication on the drying process. As previously mentioned, a high or low drying rate can be due to where in the drying process the samples are (figure 2.1) and not an accurate description of how efficient the heat transfer is.

An additional issue worth highlighting regards the dryer's inside temperature. The drying chamber's temperature is investigated to ensure that different heat levels are not the major reason influencing the drying rate between different experiments. It is beneficial for the comparison between scenarios to make sure that the same starting temperature is reached before putting the trays in. If this is done, then the temperature variation between the different scenarios can be attributed to the internal fans and amount of samples being dried and not because of different starting temperatures.

Since the thermocouples display abnormalities their precision are tested by setting them in a warm water bath. The thermocouples differs with at most 1.3 °C and the data abnormalities being because of damaged thermocouples is henceforth eliminated. The reason for the flaws in the temperature data collection is instead attributed to an issue

with the Campbell Scientific CR1000 data logger and AM16/32B multiplexer. Lastly, since inlet A scenario **A:1:2.1** is considered the optimal setup, there is a necessity to test **A:1:2.1_50.samples** to see if another local optimum can be found once the chamber is fully loaded.

6 Conclusion

In conclusion, using inlet A is optimal if an even drying process is wanted. For a higher drying rate, inlet B is proven to give better results. For inlet A it is enough to use one fan on the short side nearest the outlet of the chamber to ensure a good drying rate and even drying process. If an even process and high drying rate is to be achieved with inlet B, then two fans are required where one needs to be located below the inlet. The second fan is proven to give good results when placed at a centred height, not too far away from the first fan and on the long side opposite of the outlet. When implementing these findings in a solar dryer thoughts should be given to the risk of internal fans malfunctioning and if a heat storage is to be incorporated. These factors together with the technical aspect influences the solar dryer's design.

As seen for both inlets, increasing the airflow of the internal fans increases the drying rate of the trays while decreasing the samples water activity levels. This shows that an increased internal airflow ensures better heat transfer inside the drying chamber and results in shorter drying time.

6.1 Future research

The findings of this project should be implemented in the solar dryer shown in figure 3.2. This to get factual results and an indication of the solar dryer's improved efficiency when these finding are applied. Furthermore, it should be investigated how varying the net flow of the drying chamber together with the internal airflow affects the drying process. The possible benefits of having different flows on the individual fans inside the chamber and how changing their airflow throughout the drying process should be looked into. The reason for looking into this is that it could result in an even higher drying rate and uniform drying process while keeping the power use down. If this is implemented it will need to be automated to ensure that it is an attractive design feature for the customers.

Further research should include how the drying rate and drying process is affected depending on the tray placement. In other words, it should be investigated if it is possible for the tray placement to create a turbulent environment, increasing the drying rate and resulting in an even drying process without having to use external power in the form of internal fans. In addition, an analysis on the possibility of reducing the number of internal fans by instead creating an even drying process through diffusion of the incoming air should be conducted. If this shows promise then a simpler solar dryer design can be obtained, keeping the design cost and complexity at a minimum.

References

Andersson, M., Andersson, E., Baral, B., Davidsson, H., Lhendup, T. and P., P. O. (2020). SolarFood: Reducing post-harvest losses through improved solar drying. *Application to Swedish Scientific Council (VR)*. Application: 2020-04071.

Basnet, A., Khadka, N., Dhungana, G. and Pradhanang, A. (2020). Development and feasibility study of a mixed-mode solar dryer for Bankariya, Hetauda, Province-3, Nepal. *Kathmandu University Journal of Science, 14*(2). http://old.ku.edu.np/kuset/vol14_no2/basnet_vol_14_No_2_2020.pdf.

Bengtsson, G. V. and Döhlen, B. (2016). *Performance Testing of a Solar Thermal Fruit Dryer- A Case Study to Reduce Food Waste in Mozambique* [Master Thesis, Architecture and Built Environment].

Bhattarai, D. R. (2018). Postharvest horticulture in Nepal. *Horticulture International Journal, (2)*6, 458-460. doi: 10.15406/hij.2018.02.00096.

Castillo-Téllez, M., Pilatowsky-Figueroa, I., López-Vidaña, E. C., Sarracino-Martínez, O. and Hernández-Galvez, G. (2016). Dehydration of the red chilli (*Capsium annuum* L., costeño) using an indirect-type forced convection solar dryer. *Applied Thermal Engineering, 114*, 1137-1144. https://doi.org/10.1016/j.applthermaleng.2016.08.114.

Dong Chen, X. and Patel, K. C. (2008). Biological changes during food drying processes. In Dong Chen, X. and Mujumdar, A. S. (Eds.), *Drying Technologies in Food Processing* (pp. 90-112). Wiley-Blackwell. ISBN: 1-4051-5763-1.

Federation of Nepalese Chambers of Commerce and Industry (2013). *Agriculture*. Federation of Nepalese Chambers of Commerce and Industry [FNCCI]. Retrieved July 09, 2021, from https://www.fncci.org/agriculture-148.html.

Folaranmi, J. (2008). Design, Copnstruction and Testingof Simple Solar Maize Dryer. *Leonardo Electronic Journal of Practices and Technologies*(13), 122-130. http://193.226.7.140/lejpt/A13/122_130.pdf.

Fuller, R. J., Aye, L. and Zahnd, A. (2007). *Evaluation of a solar dryer in a high altitude area of Nepal*.ANZSES Solar. https://researchrepository.murdoch.edu.au/id/eprint/12780/1/solar_dryer_in_a_high_altitude_area.pdf.

Islam, M. K., Karim, M. S., Begum, N. N. and Uddin, K. Z. (2018). Fabrication and Performance Study of a Direct Type Solar Dryer. *International Journal of Scientific & Engineering Research, 9*(2), 565-569. https://www.researchgate.net/publication/323868160_Fabrication_and_Performance_Study_of_a_Direct_Type_Solar_Dryer.

Johansson, P. and Svensson, A. (1999). *Metoder för mätning av luftflöden i ventilationsinstallationer*. Byggforskningsrådet.

Kendall, P., DiPersio, P. and Sofos, J. (2004). Preparation-Drying Vegetables. *Food and Nutrition series*(no. 9.308). https://mountainscholar.org/bitstream/handle/10217/195050/AEXT_ucsu2062293082004.pdf?sequence=1.

Nwakuba, N. R., Asoegwu, S. N. and Nwaigwe, K. N. (2016). Energy requirements for drying of sliced agricultural products: A review. *CIGR Journal, 18*(2). https://cigrjournal.org/index.php/Ejounral/article/view/3605/2350.

Papade, C. and Boda, M. A. (2014). Design & Development of Indirect Type Solar Dryer with Energy Storing Material. *International Journal of Innovative Research in Advanced Engineering, 1*(12), 109-114. https://www.researchgate.net/publication/312589828_Design_Development_of_Indirect_Type_Solar_Dryer_with_Energy_Storing_Material.

Probert, A. (2021). [Unpublished Picture].

Rose, L. E., Karan, P. P., Proud, R. R. and Zuberi, M. (2021). *Nepal*. Encyclopedia Britannica. Retrieved July 08, 2021, from https://www.britannica.com/place/Nepal.

Rosengren, A. (2017). *Inläggning, gravning, syrning och konservering* (Rapport 8 del 1). Swedish Food Agency. https://www.livsmedelsverket.se/globalassets/publikationsdatabas/rapporter/2017/rikshanteringsrapport_inlaggning-gravning-syrning-och-konservering-livsmedelsverket-rapport-8-2017del-1.pdf.

Shafiur Rahman, M. and Perera, C. O. (2007). Drying and Food Preservation. In Shafiur Rahman, M. (Ed.), *Handbook of Food Preservation* (2nd ed., pp. 403-432). CRC Press, Taylor and Francis Group. ISBN-13: 978-1-57444-606-7.

Shakya, S., Pant Birendra, P. and Jha, V. K. (2019). Determination of the optimal tilt angle for a tilted solar panel in Kathmandu, Nepal using isotropic model. *Research Journal of Physical Sciences, 7*(2). http://isca.me/PHY$_SCI/Archive/v7/i2/2.ISCA-RJPS-2018-014.pdf$.

Subedi, G. D., Durga, M. and Gautam, D. M. (2019). Effect of hot air temperature on mechanical properties of dried apples, *Journal of Food Engineering, 64*(3),307-314. https://doi.org/10.1016/j.jfoodeng.2003.10.014.

Swedish Food Agency (2021). *Kontroll av mikrobiologiska hälsorisker*. Swedish Food Agency. Retrieved July 19, 2021, from https://kontrollwiki.livsmedelsverket.se/artikel/113/kontroll-av-mikrobiologiska-halsorisker.

Team Engineering (2019). *Pros & Cons: Wood as a building Material*. Team Engineering Building Inspection & Design. Retrieved July 27, 2021, from https://myteamengineering.com/pros-cons-wood-as-a-building-material/.

Tiwari, G., Tiwari, A. and Shyam (2016). *Handbook of Solar Energy*. Springer Science+Business Media Singapore. doi: 10.1007/978-981-10-0807-8_1.

Youcef-Ali, S., Moummi, N., Desmons, J. Y., Abene, A., Messaoudi, H. and Le Ray, M. (2001). Numerical and experimental study of dryer in forced convection. *International Journal of Energy Research, 25*(6), 537-553. https://doi.org/10.1002/er.707.

7 Appendix

7.1 Calculation of the outlet's covered area for setup using inlet B

To calculate how much of the outlet area the tray covers equation 7.1 is used. This only refers to the outlet being used when experimenting on scenarios using inlet B.

$$\begin{aligned} \text{Area} = \text{width } (w) \cdot \text{length } (l) &= 1 \text{ cm} \cdot 8.5 \text{ cm} = 8.5 \text{ cm}^2 \\ \% \text{ of the inlet hole covered} &= \frac{8.5 \text{ cm}^2}{79 \text{ cm}^2} \approx 11 \ \% \end{aligned} \tag{7.1}$$

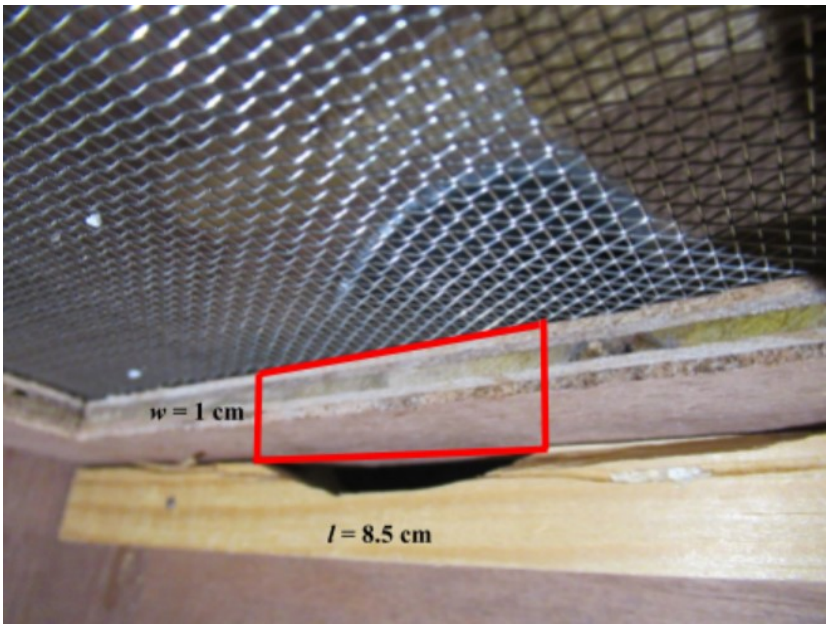

Figure 7.1: The covered area of the outlet in the setup using inlet B and the suggested geometrical shape (red) used to calculate its approximate area.

7.2 Possible measurement error for airflow calculations

According to the standard given by Johansson and Svensson (1999) the thermal anemometer probe is required to be calibrated at the prevailing temperature inside the tube. If this is not done, and for instance the instrument is calibrated for a temperature of 20 °C and measurements are made at 30 °C, a measuring error of 5 % to 10 % can be obtained. This calibration is omitted since the air velocity measurements are used solely to approximate the dryer's environment and not to draw any conclusions, rendering the error margin arising from the lack of temperature calibration trivial.

7.3 Detailed lab instructions

1. Start the data logger to record at every minute the temperature at the different locations of the drying chamber.
2. Turn on the heating lamps and allow for the chamber to warm up.
3. Depending on the experiment, slice $24 \cdot 3$ or $50 \cdot 3$ apple pieces of a thickness of 0.3 cm.
4. Measure the water activity for all samples of tray 1. Repeat for tray 2 and tray 3.
5. Divide tray 1 into 3 sections and place the samples accordingly to figure 7.2a/7.2b. Repeat for tray 2 and tray 3.
6. Weigh the samples for each section of tray 1 collectively before placing them back on the tray. Repeat for tray 2 and tray 3.
7. Measure the diameter for each of the samples.
8. Sum up the active area and weight of each section and for each tray.
9. Take pictures of tray 1, tray 2 and tray 3 once the samples are placed.
10. Put the trays in the drying chamber.
11. Measure the air velocity out every hour.
12. Measure the relative humidity in the outgoing air every hour.
13. Once the experiment is completed, photograph tray 1, tray 2 and tray 3.
14. Weigh the final sum of the samples for each section of tray 1. Repeat for tray 2 and tray 3.
15. Measure the water activity for all samples of tray 1. Repeat for tray 2 and tray 3.

7.3.1 Open experiment

1. Repeat step 1 to 9 of previous instructions.
2. Measure the diameter and weigh the five selected samples of tray 1 before placing them back. Repeat this step for tray 2 and tray 3.
3. Put the trays in the drying chamber.
4. For all trays, weigh each of the selected samples every two hour.
5. Conduct step 11 to 15 of previous instruction

If there is no change in the outgoing air velocity and RH measurements then these can be taken once per experiment. If there is a change they should be taken continuously.

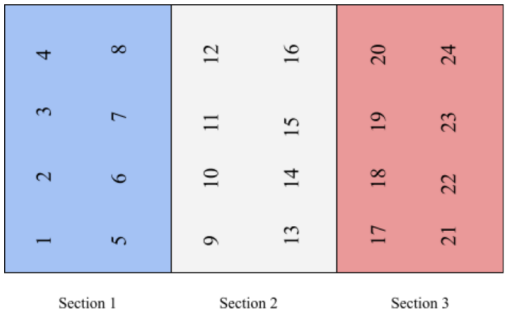

Figure 7.2a: Diagram showing the labelling of the samples for a tray with 24 samples.

Figure 7.2b: Diagram showing the labelling of the sample for a tray with 50 samples.

LUND UNIVERSITY

Dept of Architecture and Built Environment: Division of Energy and Building Design
Dept of Building and Environmental Technology: Divisions of Building Physics and Building Services